Hsc70 chaperone activity underlies Trio GEF function in axon growth and guidance induced by netrin-1

Jonathan DeGeer,[1,2] Andrew Kaplan,[3] Pierre Mattar,[4] Morgane Morabito,[1,2] Ursula Stochaj,[5] Timothy E. Kennedy,[1,3] Anne Debant,[6] Michel Cayouette,[1,4,7] Alyson E. Fournier,[1,3] and Nathalie Lamarche-Vane[1,2]

[1]Department of Anatomy and Cell Biology, McGill University, Montreal, Quebec H3A 0C7, Canada
[2]The Research Institute of McGill University Health Centre, Montreal, Quebec H4A 3J1, Canada
[3]Department of Neurology and Neurosurgery, McGill University, Montreal, Quebec H3A 2B4, Canada
[4]Cellular Neurobiology Research Unit, Institut de Recherches Cliniques de Montréal, Montreal, Quebec H2W 1R7, Canada
[5]Department of Physiology, McGill University, Montreal, Quebec H3G 1Y6, Canada
[6]Centre de Recherche de Biochimie Macromoléculaire, Centre National de la Recherche Scientifique, UMR5237, University of Montpellier, Montpellier 34293, France
[7]Department of Medicine, Université de Montréal, Montreal, Quubec H3T 1J4, Canada

During development, netrin-1 is both an attractive and repulsive axon guidance cue and mediates its attractive function through the receptor Deleted in Colorectal Cancer (DCC). The activation of Rho guanosine triphosphatases within the extending growth cone facilitates the dynamic reorganization of the cytoskeleton required to drive axon extension. The Rac1 guanine nucleotide exchange factor (GEF) Trio is essential for netrin-1–induced axon outgrowth and guidance. Here, we identify the molecular chaperone heat shock cognate protein 70 (Hsc70) as a novel Trio regulator. Hsc70 dynamically associated with the N-terminal region and Rac1 GEF domain of Trio. Whereas Hsc70 expression supported Trio-dependent Rac1 activation, adenosine triphosphatase–deficient Hsc70 (D10N) abrogated Trio Rac1 GEF activity and netrin-1–induced Rac1 activation. Hsc70 was required for netrin-1–mediated axon growth and attraction in vitro, whereas Hsc70 activity supported callosal projections and radial neuronal migration in the embryonic neocortex. These findings demonstrate that Hsc70 chaperone activity is required for Rac1 activation by Trio and this function underlies netrin-1/DCC-dependent axon outgrowth and guidance.

Introduction

The proper wiring of the central nervous system (CNS) is imperative for normal physiological function and survival. During development, the extension and pathfinding of neurons of the CNS is governed in part by environmental guidance cues (Tessier-Lavigne and Goodman, 1996; Guan and Rao, 2003; Huber et al., 2003). Molecular signals initiated by these cues are transduced intracellularly by means of conserved receptors expressed at the distal axon growth cone, ultimately resulting in modulation of the actin cytoskeleton (Lowery and Van Vactor, 2009). Netrins constitute a family of axon guidance cues that are required for proper neural specification (Kennedy et al., 1994; Serafini et al., 1996; Bashaw and Klein, 2010). To date, netrin-1 was found to signal through at least four distinct families of transmembrane receptors: the Deleted in Colorectal Cancer (DCC) family (DCC and neogenin), Down syndrome cell adhesion molecule, the UNC-5 family, and amyloid precursor protein (Keino-Masu et al., 1996; Ackerman et al., 1997; Leonardo et al., 1997; Ly et al., 2008; Liu et al., 2009; Rama et al., 2012). During development of the spinal cord and cerebral cortex of vertebrates, netrin-1 exerts its attractive functions through the receptor DCC (Kennedy et al., 1994; Keino-Masu et al., 1996; Richards et al., 1997). In humans, mutations of the *DCC* gene have been associated with congenital mirror movements (Srour et al., 2010), and small nucleotide polymorphisms within the genes encoding *DCC* and *netrin-1* have been associated with schizophrenia (Grant et al., 2012), Parkinson's disease, and amyotrophic lateral sclerosis (Lesnick et al., 2008; Lin et al., 2009). Upon netrin-1 stimulation, DCC becomes highly phosphorylated on serine, threonine, and tyrosine residues (Meriane et al., 2004). In particular, phosphorylation of rat DCC at Tyr^{1418} by Src family kinases is required for netrin-1–mediated axon outgrowth and guidance in vertebrates (Li et al., 2004; Liu et al., 2004; Meriane et al., 2004).

Rho family GTPases are molecular switches that have been well characterized as modulators of cytoskeletal dynamics and cellular motility by cycling between an inactive GDP-bound and active GTP-bound state (Jaffe and Hall, 2005). In the context of axon growth and pathfinding, the recruitment and localized activation of the Rho GTPases Rac1, Cdc42, and RhoA are imperative for translating guidance cues into cytoskeletal rearrangements within

Correspondence to Nathalie Lamarche-Vane: nathalie.lamarche@mcgill.ca

Abbreviations used in this paper: ANOVA, analysis of variance; CRIB, Cdc42/Rac interactive binding; CNS, central nervous system; DCC, Deleted in Colorectal Cancer; DIV, days in vitro; GEF, guanine nucleotide exchange factor; GEFD, GEF domain; IP, immunoprecipitated.

The Rockefeller University Press $30.00
J. Cell Biol. Vol. 210 No. 5 817–832
www.jcb.org/cgi/doi/10.1083/jcb.201505084

the extending growth cone (Li et al., 2002; Barallobre et al., 2005; Lowery and Van Vactor, 2009; Antoine-Bertrand et al., 2011; DeGeer and Lamarche-Vane, 2013). Downstream of netrin-1/DCC, Rac1 becomes activated in neurons and drives axonal extension, whereas RhoA activity is inhibited (Li et al., 2002; Shekarabi and Kennedy, 2002; Briançon-Marjollet et al., 2008; Moore et al., 2008). Oversight of Rho GTPase nucleotide cycling is performed by regulatory proteins: guanine nucleotide exchange factors (GEFs) enhance the GTP-bound state (Cook et al., 2014; Laurin and Côté, 2014), whereas GTP hydrolysis is catalyzed by GTPase-activating proteins (Tcherkezian and Lamarche-Vane, 2007). Additionally, guanine nucleotide dissociation inhibitors bind to Rho GTPases and restrict them in an inactive state in the cytoplasm, preventing them from associating with their downstream effectors (Olofsson, 1999). In recent years, the GEFs DOCK180 and Trio have been shown to mediate Rac1 activation downstream of netrin and DCC in mammalian systems (Briançon-Marjollet et al., 2008; Li et al., 2008). Trio contains two Dbl homology/Pleckstrin homology GEF domains (GEFDs) and a serine/threonine kinase domain for which a substrate has yet to be identified (Debant et al., 1996). Trio has activity toward both RhoG and Rac1 via its first GEFD (GEFD1), whereas the second GEFD activates RhoA in vitro (Debant et al., 1996; Bellanger et al., 1998; Blangy et al., 2000). Trio is highly enriched in the mammalian brain where five Trio isoforms containing the GEFD1 are generated by alternative splicing (Portales-Casamar et al., 2006). Trio-null mice die between embryonic day 15.5 (E15.5) and birth and display a general impairment of netrin-1– and DCC-dependent neuronal projections in the spinal cord and brain (O'Brien et al., 2000; Briançon-Marjollet et al., 2008). Specifically, in the brain Trio-null embryos lack anterior commissures, and notably DCC-positive projections in the corpus callosum and internal capsule are misguided (Briançon-Marjollet et al., 2008). We have recently shown that netrin-1 promotes the Src kinase-dependent phosphorylation of $Trio^{Y2622}$ and a concomitant coassociation with DCC in cortical growth cones occurring when Rac1 activation peaks (DeGeer et al., 2013). We also observed that Trio promotes the enrichment of surface DCC at cortical neuronal growth cones in a $Trio^{Y2622}$-dependent manner (DeGeer et al., 2013). These findings demonstrated the importance of $Trio^{Y2622}$ phosphorylation in the regulation of netrin-1– and DCC-mediated cortical axon outgrowth. Despite these observations, the mechanisms governing Trio localization and activation downstream of netrin-1/DCC are unknown. In this work we provide evidence that the chaperone activity of Hsc70 permits Rac1 activation by Trio in the developing cerebral cortex. In addition, we show that Hsc70 function is required for proper Trio and DCC localization in cortical growth cones treated with netrin-1. We correlate the chaperone-mediated activation of Rac1 by Trio with the regulation of DCC plasma membrane insertion within the growth cones of cortical neurons and demonstrate Hsc70's requirement for axon outgrowth and guidance induced by netrin-1. In this way we link cytoskeletal proteins with the regulation of an axon guidance receptor and describe a novel function for the chaperone Hsc70 during development.

Results

The molecular chaperone Hsc70 associates with Trio in the developing cerebral cortex

To characterize the molecular mechanisms governing Trio regulation during netrin-1/DCC signaling, we used a proteomic approach and identified Hsc70 as a novel Trio-associated protein in extracts of netrin-1–treated rat E17.5 cerebral cortices. To validate the mass spectrometry result, Trio was immunoprecipitated (IP) from cortical tissue extracts and coassociated proteins were analyzed by Western blot. We found that Hsc70 interacted with Trio, whereas the highly homologous chaperone Hsp70 failed to do so (Fig. 1 A). To determine whether the association between Trio and Hsc70 was netrin dependent, rat cortices were treated with netrin-1 for 5 to 30 min before harvesting. Trio and Hsc70 coassociation in cell extracts peaked 5 min after netrin-1 stimulation and decreased after 15 and 30 min (Fig. 1, B and C). FAK was activated (pFAK) after 5 min of netrin-1 treatment and activation was sustained for at least 30 min, as reported previously (Fig. 1 B; DeGeer et al., 2013).

We next investigated the degree of endogenous coassociation of Trio and Hsc70 in dissociated cortical neurons by indirect immunofluorescence. Neurons were treated with netrin-1, and then fixed and stained with antibodies against Trio and Hsc70 (Fig. 1 D). Confocal microscopy was performed and the mean Pearson's correlation coefficient between Trio and Hsc70 was generated at both cortical growth cones and axon shafts to assess the degree of coassociation. By this means, we observed a basal colocalization between Trio and Hsc70 in the cortical growth cones ($r = 0.50 \pm 0.02$; Fig. 1, D and E). Netrin-1 treatment significantly increased the colocalization of Trio and Hsc70 within growth cones after 5 min ($r = 0.62 \pm 0.02$, $P < 0.0007$), whereas the colocalization returned to basal levels after 15 min of netrin-1 treatment ($r = 0.47 \pm 0.02$, $P < 0.0001$; Fig. 1, D and E). The basal colocalization of Hsc70 and Trio in axon shafts was similar to the growth cones ($r = 0.51 \pm 0.02$); however, netrin-1 application for either 5 or 15 min resulted in no significant modulation of the association ($r = 0.48 \pm 0.03$ and $r = 0.42 \pm 0.02$, $P > 0.05$; Fig. 1, F and G). In summary, we identified Hsc70 as a novel Trio-associated protein in embryonic cortical tissues and demonstrate that the netrin-1–induced coassociation occurs preferentially in cortical growth cones versus axons.

Hsc70 facilitates Trio-dependent Rac1 activation and cortical axon outgrowth in a chaperone-dependent manner

To delineate the regions of Trio permitting the association with Hsc70, GFP-Trio deletion mutants were expressed in HEK293 cells and the interaction with Hsc70 was assessed by coimmunoprecipitation (Fig. 2, A and B). In this assay, full-length GFP-Trio basally associated with endogenous Hsc70, and the C-terminal truncation of Trio, lacking the RhoA GEF and kinase domains resulting in the Trio 1–1813 fragment, did not reduce the association with Hsc70 relative to immunoprecipitation efficiency (Fig. 2, A–C). On the contrary, the shorter fragments of Trio comprising the Sec14 domain (Trio 1–232) or GEFD1-SH3 (Trio 1203–1813) highly associated with Hsc70 (Fig. 2, B and C). Intriguingly, the intermediate fragment containing the Sec14 domain but lacking the GEFD1-SH3 domain (Trio 1–1203) did not associate with Hsc70 in an elevated manner (Fig. 2, B and C). These results suggest that Hsc70 association with Trio may be mediated in part by the N terminus and GEFD1-SH3 of Trio, though both regions may differentially cooperate to accommodate association in the context of full-length or neural Trio isoforms that have intact N-terminal domains (Portales-Casamar et al., 2006).

Because the GEFD1 of Trio highly associated with endogenous Hsc70, we next sought to determine whether Hsc70 mod-

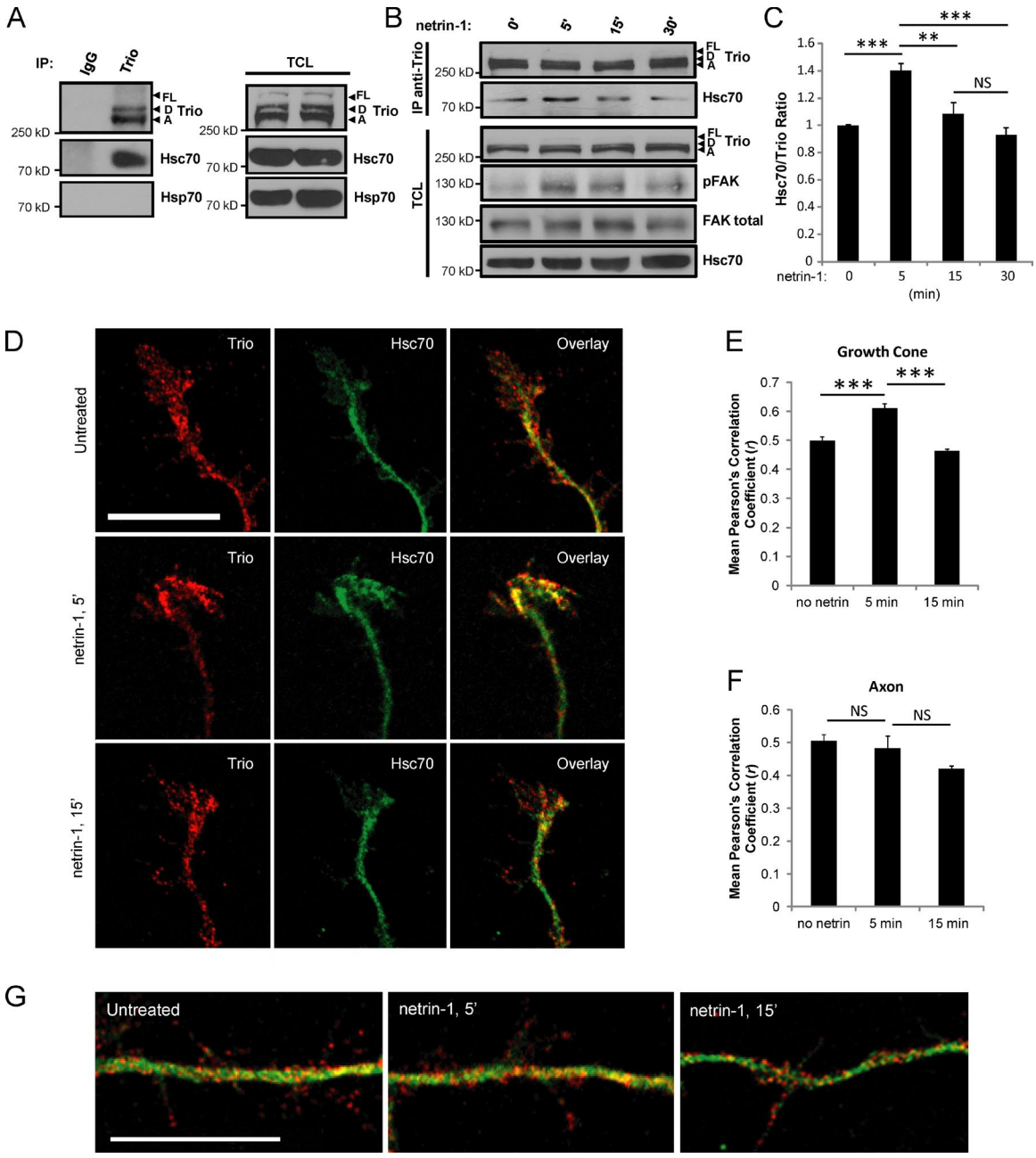

Figure 1. **The molecular chaperone Hsc70 associates with Trio in the developing cerebral cortex.** (A) Trio was IP from lysates of isolated E17.5 rat cortices with anti-Trio antibodies or rabbit IgG as a control. IP proteins and total cell lysates (TCL) were resolved by SDS-PAGE and immunoblotted with the indicated antibodies. Trio isoforms: FL, full length; D, Trio-D; A, Trio-A. (B) Isolated E17.5 rat cortices were stimulated with netrin-1 for the indicated times. Trio isoforms were IP and Hsc70 coIP with Trio was assessed by immunoblotting. Netrin-1 stimulation of DCC-induced signaling pathways was assessed by evaluating FAK phosphorylation (Y861) in total cell lysates (TCL). (C) Densitometric analysis of Hsc70 coIP with Trio from B. Error bars indicate the SEM (n = 5; NS, $P > 0.05$; **, $P < 0.001$; ***, $P < 0.0001$; one-way ANOVA, Bonferroni's multiple comparisons test). (D and G) Dissociated E17.5 rat cortical neurons were stimulated with netrin-1 for 5 and 15 min before fixation. Endogenous Trio and Hsc70 localization were assessed by indirect immunofluorescence and confocal microscopy. Bars, 15 µm. (E and F) The mean Pearson's correlation coefficient between green (Hsc70) and red (Trio) channels within the growth cone (D and E) or axon shaft (F and G) was calculated with Metamorph software. Error bars indicate the SEM (>48 neurons were assessed per condition, from three independent experiments; NS, $P > 0.05$; **, $P < 0.001$; ***, $P < 0.0001$; one-way ANOVA, Bonferroni's multiple comparisons test).

ulates the Rac1 GEF activity of Trio. We performed pull-down assays with the Cdc42/Rac interactive binding (CRIB) domain of PAK fused to GST to assess the level of active GTP-Rac1 in HEK293 cell extracts (Briançon-Marjollet et al., 2008; Picard et al., 2009). As expected, Trio overexpression resulted in a significant increase in Rac1-GTP levels ($P = 0.0003$), whereas the expression of Hsc70 had no significant effect on Rac-GTP levels alone ($P = 0.28$; Fig. 2, D and E). Increasing levels of GFP-Hsc70 coexpression with GFP-Trio resulted in enhanced Trio-dependent Rac-GTP induction with low levels of Hsc70 ($P < 0.03$), whereas higher levels of Hsc70 expression did not significantly augment Trio-induced Rac1 activation ($P = 0.44$; Fig. 2, D and E). To examine whether Hsc70 chaperone activity is required to modulate the activation of Rac1 by Trio, the dominant-negative

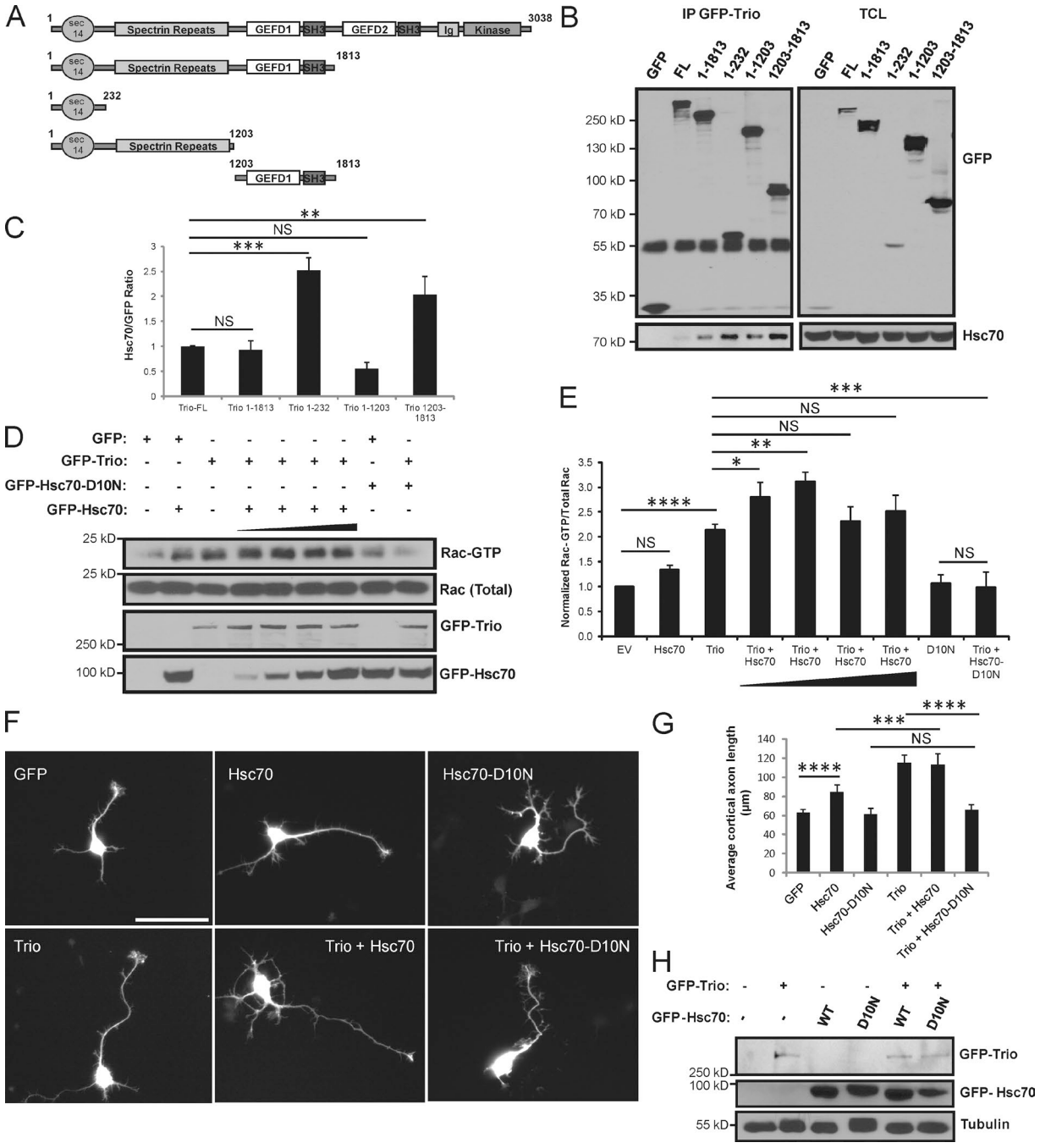

Figure 2. **Hsc70 facilitates Trio-dependent Rac1 activation and cortical axon outgrowth in a chaperone-dependent manner.** (A) Schematic of Trio domain structure. (B) Trio constructs were transfected into HEK293 cells as indicated. GFP-Trio proteins were IP from cell lysates and Hsc70 coIP with Trio was detected by immunoblotting. TCL, total cell lysates. (C) Densitometric analysis of Hsc70 coIP with GFP-Trio from B. Error bars indicate the SEM (n = 3; NS, P > 0.05; **, P < 0.001; ***, P < 0.0001; one-way ANOVA, Bonferroni's multiple comparisons test). (D) HEK293 cells were transfected with the indicated constructs and with increasing amounts of GFP-Hsc70 plasmid. GTP-loaded Rac1 was pulled down from protein lysates by GST-CRIB. GTP-bound Rac1, total Rac1, and the indicated proteins were detected by immunoblotting. (E) Densitometric ratio of GTP-bound Rac1/total Rac1 normalized to the vector control. Error bars indicate the SEM (n = 4; NS, P > 0.05; *, P < 0.05; ***, P < 0.0001; one-way ANOVA, Bonferroni's multiple comparisons test). (F) Dissociated E17.5 rat cortical neurons were electroporated with the indicated constructs and a GFP reporter. Bar, 50 µm. (G) The mean axon lengths of GFP+ neurons were calculated manually with Metamorph software (>54 axons per condition from three independent experiments). Error bars indicate the SEM (NS, P > 0.05; **, P < 0.001; ***, P < 0.0001; one-way ANOVA, Bonferroni's multiple comparisons test). (H) Representative protein expression of electroporated constructs in E17.5 cortical neurons from F and G. WT, wild-type Hsc70; D10N, Hsc70^{D10N}.

and chaperone-dead (ATPase-deficient) Hsc70^{D10N} was introduced and Rac1-GTP pull-downs were performed. Although GFP-Hsc70^{D10N} expression alone had no effect on basal Rac-GTP levels, the coexpression of GFP-Hsc70^{D10N} with Trio abolished Trio-dependent Rac1 activation (Fig. 2, D and E). These results demonstrate that Trio Rac1 GEF activity is regulated by Hsc70 in a chaperone activity-dependent manner.

We have previously reported that exogenous Trio expression in dissociated cortical neurons increases axon length in a Rac1 GEF-dependent manner, thereby serving as a readout of

Trio function (DeGeer et al., 2013). We applied this model to assess whether Hsc70 functionally regulates Trio-dependent axon outgrowth. Dissociated cortical neurons were electroporated with constructs encoding GFP and either GFP-Hsc70 or GFP-Hsc70^{D10N} alone or with GFP-Trio. After 2 d in culture the neurons were fixed and imaged and the mean axon length of GFP-positive (GFP$^+$) cells was determined (Fig. 2, F and G). Although expression of GFP-Hsc70 or Trio alone resulted in a significant increase in axon length relative to control cells ($P < 0.0001$), coexpression of Hsc70 and Trio did not further enhance the mean axon length relative to Trio-expressing neurons ($P = 0.97$; Fig. 2, F and G). Axon lengths of GFP-Hsc70^{D10N}–expressing neurons were not significantly different from GFP-expressing neurons, whereas coexpression of GFP-Hsc70^{D10N} with Trio abrogated Trio-dependent enhanced axon extension ($P < 0.0001$; Fig. 2, F and G). To rule out possible down-regulation or degradation of proteins, the expression of GFP-tagged proteins was verified by immunoblotting (Fig. 2 H). Altogether, these data demonstrate that Rac-GTP induction by Trio is modulated by Hsc70 chaperone activity, which is required for Trio-stimulated axon extension in cortical neurons.

Hsc70 is required for the netrin-1–induced enrichment of Trio at the growth cone periphery

Because Hsc70 is a molecular chaperone, we assessed whether it may function to regulate Trio localization within cortical growth cones. To first establish Trio localization, cortical neurons were treated with netrin-1 for 5 min, and then fixed and stained (Fig. 3 A). Trio and F-actin growth cone localizations were assessed and the intensity of each signal was measured along a 10-µm segment of the distal growth cone (Fig. 3 A, right). Upon netrin-1 treatment, the intensity of Trio shifted to the growth cone periphery compared with untreated growth cones, similar to F-actin (Fig. 3, A and B).

We next down-regulated endogenous Hsc70 in neurons by electroporation of synthetic siRNA targeting the 5′-UTR of rat Hsc70 along with GFP cDNA as a transfection marker. Neurons were fixed and immunostained for endogenous Hsc70, and the level of Hsc70 present in GFP$^+$ neurons versus GFP-negative neurons was assessed by indirect immunofluorescence (Fig. 3, C and D). In this manner, we observed a 60% reduction in the total level of Hsc70 in GFP$^+$ neurons relative to nontransfected neurons (Fig. 3 D). Subsequently, Trio localization was assessed within the growth cones of dissociated neurons electroporated with either control or Hsc70 siRNA and stimulated with netrin-1 for 5 min. In the absence of netrin-1, Trio localization was dispersed throughout the growth cones of control neurons with reduced incidence of compartmentalization in the growth cone periphery (15.17 ± 4.30%; Fig. 3, E–G). Similarly, in Hsc70-depleted neurons Trio was largely dispersed throughout the growth cones and a lower proportion displayed a peripheral Trio localization (Periphery: 6.16 ± 0.32%; Fig. 3, E–G). Netrin-1 application for 5 min resulted in an increase in the proportion of growth cones with peripheral Trio localization (59.25 ± 5.46%, $P < 0.001$; Fig. 3, E–G). In contrast, Hsc70-depleted neurons displayed no significant change in Trio localization (8.33 ± 2.08%, $P = 0.23$; Fig. 3, E–G). Together with the previous finding that Hsc70 is required for Trio-dependent axon outgrowth, this data supports a hypothesis whereby Hsc70 regulates Trio function in the extending growth cone by regulating Trio localization.

Hsc70 associates with a DCC multiprotein signaling complex

Because Trio and DCC coassociate in cortical neurons treated with netrin-1 (DeGeer et al., 2013), we next examined the interaction between Hsc70 and DCC in cortical tissues. Protein extracts from cerebral cortices treated with netrin-1 for 5, 15, and 30 min were collected; DCC was IP; and the level of Hsc70 coassociating was determined by immunoblotting (Fig. 4 A). Similar to our findings for Trio and Hsc70 interaction, the association of Hsc70 with DCC increased after 5 min of netrin-1 stimulation. However, unlike Trio, DCC remained associated with Hsc70 until after 15 min of treatment (Fig. 4, A and B). The coassociation of Trio and FAK with DCC also increased after 5 min of netrin-1 stimulation and remained elevated until 15 min after treatment (Fig. 4 A). These results show that Hsc70 is part of a DCC–Trio–FAK signaling complex induced by netrin-1 in cortical tissues.

Because chaperones function in part by regulating protein trafficking and half-life (Hartl et al., 2011), we next investigated whether Hsc70 association with DCC occurs at the plasma membrane or intracellularly. Dissociated cortical neurons were cultured for 48 h before netrin-1 treatment and subsequently processed according to a surface labeling protocol using an antibody against the extracellular domain of DCC (Fig. 4 C; Kim et al., 2005). After surface DCC isolation from cell extracts, the remaining fraction of intracellular DCC was isolated by immunoprecipitation. In this manner, Hsc70 was found to coassociate more with surface DCC relative to the intracellular-enriched DCC pool. Moreover, netrin-1 treatment enhanced the coassociation of Hsc70 with surface DCC, whereas treatment did not significantly affect Hsc70 binding with intracellular DCC relative to DCC immunoprecipitation efficiency (Fig. 4 C). Collectively, these data demonstrate that Hsc70 is associated with DCC signaling complexes in the developing cortex and that Hsc70 association is stronger with surface DCC after netrin-1 treatment.

Hsc70 chaperone activity supports surface DCC enrichment in cortical growth cones

We next investigated whether Hsc70 influences DCC surface localization in growth cones downstream of netrin-1. To assess this, dissociated cortical neurons expressing GFP-Hsc70 or the dominant-negative, ATPase-dead GFP-Hsc70^{D10N} were treated with netrin-1 for 15 min before fixation. The levels of surface DCC were assessed by indirect immunofluorescence under nonpermeabilizing conditions using antibodies against the extracellular domain of DCC (Fig. 4, D and E). In this manner, we observed that the enrichment of surface DCC at the growth cones of GFP-Hsc70– or GFP-Hsc70^{D10N}–expressing neurons was indistinguishable from control neurons (Fig. 4, D and E). Although netrin-1 treatment resulted in a maintained enrichment of surface DCC intensity at the growth cones of both control and GFP-Hsc70–expressing neurons, the enrichment of surface DCC at the growth cones of GFP-Hsc70^{D10N}–expressing neurons was significantly reduced ($P = 0.01$; Fig. 4, D and E). Notably, the netrin-1–induced activation of FAK and ERK pathways were not altered in HEK293 cells coexpressing Hsc70^{D10N}, suggesting that regulation of surface DCC localization may be independent of FAK and ERK signaling (Fig. 4, F–H). Altogether, these results show that the stabilized enrichment of DCC at the growth cone plasma membrane downstream of netrin-1 requires Hsc70 chaperone activity.

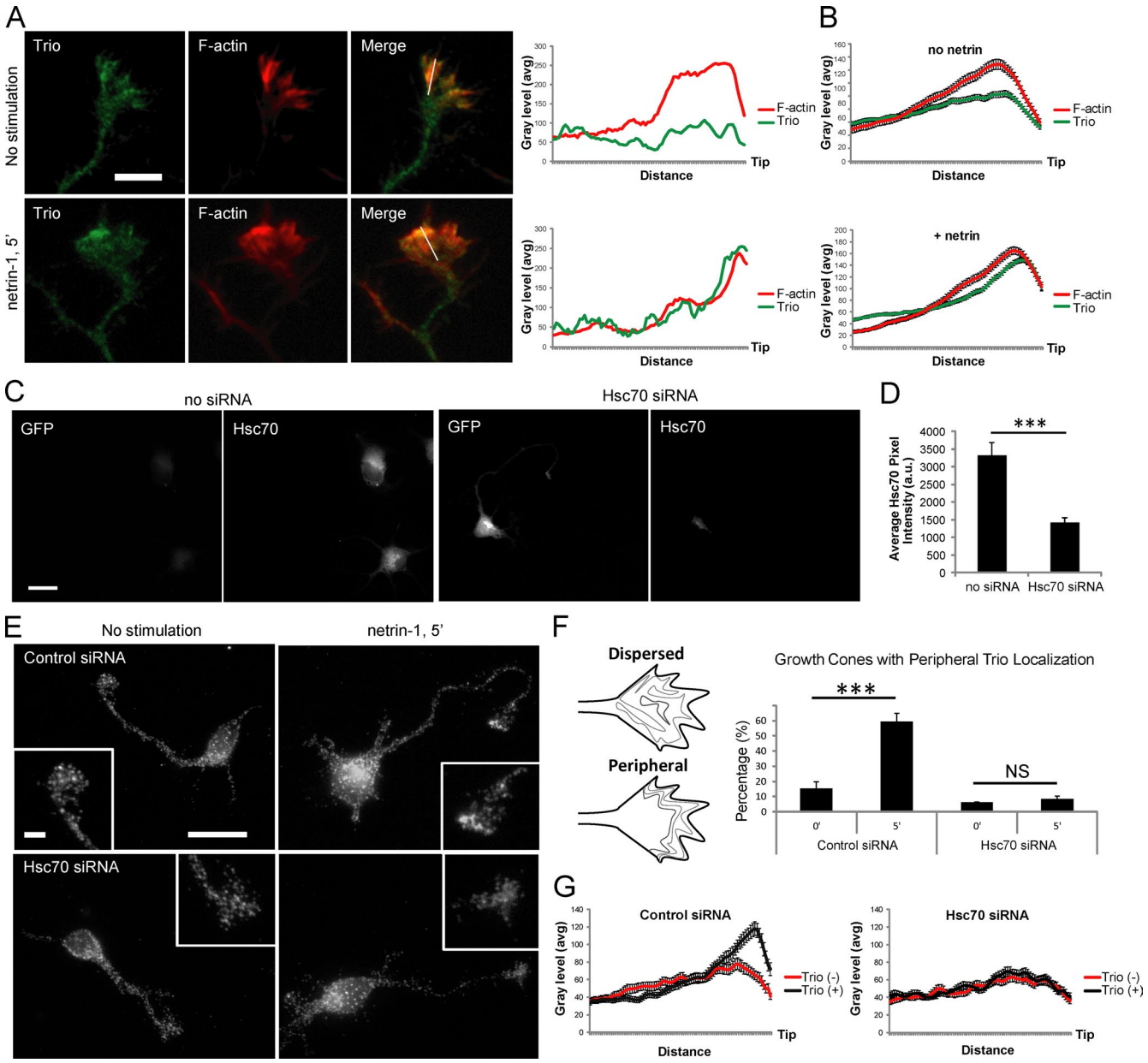

Figure 3. **Hsc70 is required for the netrin-1–induced enrichment of Trio at the growth cone periphery.** (A) Dissociated E17.5 rat cortical neurons were left untreated or stimulated with netrin-1 for 5 min before fixation. Endogenous Trio and F-actin localization were assessed by epifluorescence microscopy. Bar, 10 µm. (right) The intensity of Trio and F-actin fluorescence along a 10-µm linescan oriented in the central-to-peripheral axis of the growth cone was calculated using Metamorph software. Trio (green) and F-actin (red) pixel intensities from the adjacent images were plotted against distance. (B) The mean pixel intensity of Trio (green) and F-actin (red) along a 10-µm linescan were plotted against distance as in A. The data shown are the mean of >130 growth cones, from four independent experiments. Error bars indicate the SEM. (C) Dissociated E17.5 rat cortical neurons were electroporated with a GFP-reporter and Hsc70 siRNA. At DIV1, cultures were fixed and levels of endogenous Hsc70 were assessed by indirect immunofluorescence. Bar, 15 µm. (D) The mean pixel intensity of Hsc70 was calculated. Error bars indicate the SEM (n = 3; GFP-negative neurons = 19; GFP-positive neurons = 20; ***, $P < 0.001$; unpaired student's t test). (E) As in C, dissociated E17.5 rat cortical neurons were electroporated with a GFP-reporter and control siRNA or Hsc70 siRNA and left untreated or treated with netrin-1 for 5 min before fixation. Trio localization was assessed by indirect immunofluorescence. Bars: (main) 25 µm; (inset) 5 µm. (F, left) Schematic of Trio localization showing dispersed localization versus peripheral enrichment. (right) The proportion of electroporated neurons with growth cones harboring a distinct peripheral Trio localization was calculated for each treatment in E (>70 neurons assessed per condition, from four independent experiments). Error bars indicate the SEM (***, $P < 0.001$; unpaired student's t test). (G) As in B, the mean pixel intensity of Trio was calculated along 10-µm linescans oriented in the central-to-peripheral axis of each growth cone from E (n > 65 growth cones per condition).

Hsc70 is required for netrin-1–mediated cortical axon outgrowth and Rac1 activation

We next explored the role of Hsc70 in netrin-1–induced axon outgrowth of dissociated cortical neurons. Cortical neurons were electroporated with control or Hsc70 siRNA together with GFP cDNA and stimulated with either netrin-1 or glutamate for 24 h before fixation (Fig. 5, A and B). Although depletion of endogenous Hsc70 did not affect basal cortical axon lengths, netrin-1 treatment was insufficient to stimulate axon extension in these neurons (Fig. 5, A and B). In contrast, Hsc70-depleted neurons remained responsive to glutamate (P

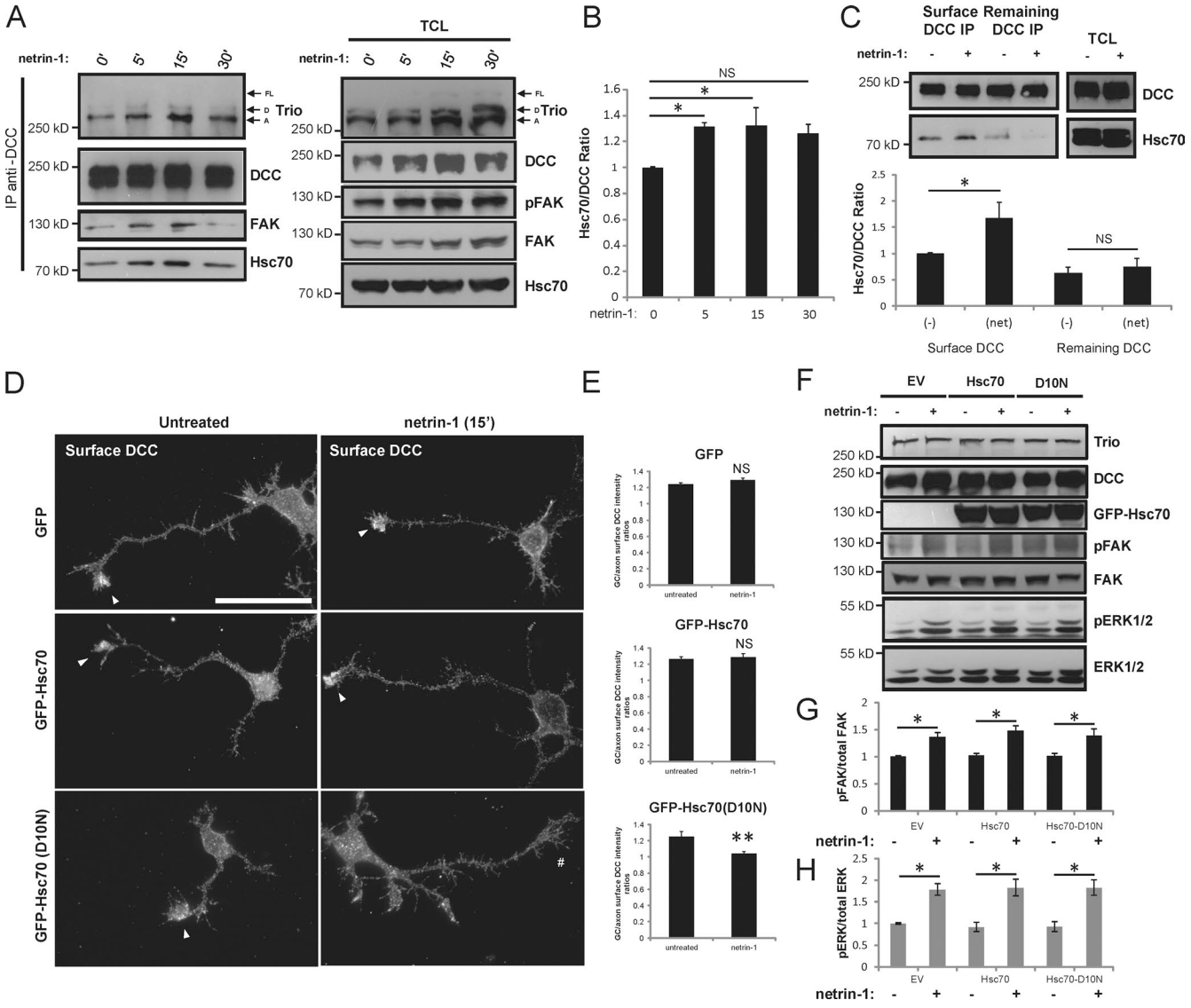

Figure 4. **Hsc70 associates with a DCC multiprotein signaling complex and supports DCC cell surface localization downstream of netrin-1.** (A) Isolated E17.5 rat cortices were stimulated with netrin-1 for the indicated times. DCC was IP and the level of Trio, FAK, and Hsc70 coIP with DCC was assessed by immunoblotting. TCL, total cell lysates. (B) Densitometric analysis of Hsc70 coIP with DCC. Error bars indicate SEM (n = 4; NS, $P > 0.05$; *, $P < 0.05$; one-way ANOVA, Dunnett's multiple comparisons test). (C) Cortical neurons were dissociated and treated with netrin-1 at DIV2, followed by surface DCC isolation. Subsequent IP of lysates depleted of surface DCC were performed and the level of Hsc70 coIP with DCC was assessed by immunoblotting. (bottom) Densitometric analysis of Hsc70 coIP with either surface or intracellular DCC. Error bars indicate SEM (n = 4; NS, $P > 0.05$; *, $P < 0.05$; unpaired student's t test). (D) Isolated E17.5 rat cortical neurons were electroporated with the indicated Hsc70 constructs. At DIV1 the neurons were treated with netrin-1 for 15 min before fixation. Surface DCC was assessed by staining with an extracellular DCC antibody under nonpermeabilizing conditions and subsequent fluorescence microscopy. Arrowhead denotes enchrichment and # denotes no enrichment. Bar, 50 µm. (E) The mean pixel intensity ratios of surface DCC at the growth cones relative to axons were calculated using Metamorph software (>54 neurons assessed per condition, from four independent experiments). Error bars indicate the SEM (**, $P < 0.01$; unpaired student's t test). (F) HEK293 cells were transfected with pRK5-DCC with empty vector (EV), GFP-Hsc70, or GFP-Hsc70^{D10N} and stimulated with netrin-1 for 5 min before lysis. Protein extracts were resolved by SDS-PAGE and the levels of active ERK1/2 and FAK were assessed by immunoblotting. (G and H) Densitometric analysis of pERK1/2 and pFAK (Y861) over total proteins from F. Error bars indicate SEM (n = 4; *, $P < 0.05$; unpaired student's t test).

< 0.03), confirming that Hsc70 depletion does not impair all mechanisms of induced axon outgrowth (Fig. 5, A and B). To verify the function of Hsc70 in netrin-1–mediated axon outgrowth, siRNA-resistant GFP-Hsc70 or GFP-Hsc70^{D10N} were expressed in Hsc70-depleted cortical neurons and stimulated with netrin-1 (Fig. 5, A and C). Reexpression of Hsc70 was sufficient to restore netrin-1–induced cortical axon extension ($P < 0.05$), whereas expression of the chaperone-dead Hsc70^{D10N} did not rescue netrin-1 sensitivity relative to untreated neurons ($P = 0.45$; Fig. 5, A and C).

To determine whether Hsc70 functions upstream or downstream of Trio during netrin-1–induced axon outgrowth, cortical neurons were depleted of endogenous Hsc70 or Trio (DeGeer et al., 2013) and expression was rescued with siRNA-resistant GFP-Trio or GFP-Hsc70 cDNAs (Fig. 5 D). In this context, GFP-Hsc70 overexpression was not sufficient to restore netrin-1–induced axon extension in Trio-depleted neurons ($P = 0.75$; Fig. 5, D and E). Conversely, when neurons were depleted of endogenous Hsc70, the overexpression of GFP-Trio restored the sensitivity of these neurons to netrin-1

and they extended longer axons (P = 0.047; Fig. 5, D and F). These results demonstrate that Hsc70 is specifically required for netrin-1–mediated cortical axon outgrowth by functioning upstream of Trio. This is in agreement with our findings that Hsc70 potentiates Trio-dependent Rac1 activation (Fig. 2 C), which is a requisite for netrin-1–induced axon extension (Li et al., 2002; Briançon-Marjollet et al., 2008).

To examine whether Hsc70 contributes to netrin-1–induced Rac1 activation, we coexpressed either Hsc70 or $Hsc70^{D10N}$ with DCC in HEK293 cells. Upon stimulation with netrin-1 for 5 min, we assessed the levels of Rac1-GTP by pull-down assays. In these studies, netrin-1 treatment of Hsc70-expressing cells led to an activation of Rac1 similar to control cells expressing DCC alone, whereas expression of $Hsc70^{D10N}$ specifically inhibited netrin-1–stimulated Rac1 activation relative to the netrin-1–treated control (P > 0.05; Fig. 5, G and H). Therefore, Hsc70 chaperone activity is necessary for netrin-1 to stimulate Rac1 activity. We propose that Hsc70 chaperone activity acting upstream of Trio during netrin-1–induced cortical axon extension is essential through its regulation of Trio Rac1 GEF activity.

Hsc70 is required for netrin-1–dependent attraction of embryonic cortical neurons

We have previously reported that Trio-null embryos have defective neural projections within the CNS, notably the netrin-1–dependent ventral projections of spinal commissural axons and DCC-positive projections of the corpus callosum and internal capsule (Briançon-Marjollet et al., 2008). In each case, a deficit in axon guidance was observed as the projected fibers were dispersed over a larger area compared with wild-type embryos (Briançon-Marjollet et al., 2008). Because Trio contributes to axon guidance in vivo (Briançon-Marjollet et al., 2008), we next evaluated the contribution of Hsc70 to netrin-1–induced chemoattraction of cortical neurons. To assess this proposed function, we used an in vitro axon guidance assay based on the Dunn chamber (Yam et al., 2009). E17.5 rat cortical neurons electroporated with control or Hsc70 siRNA with GFP cDNA were exposed to either a vehicle (PBS) or netrin-1 gradient in the Dunn chamber for at least 90 min at 2 d in vitro (DIV2; Fig. 6, A and B). Notably, a minimum of 10-µm displacement threshold was enforced for the calculated trajectory of the growth cone to be considered a "turn." As an internal control, naive cortical neurons (nonelectroporated) were also assessed. Although the mean turning angles of each PBS-treated condition did not vary significantly (P > 0.2), netrin-1 induced a robust attractive turning response for either the naive or control siRNA-electroporated neurons, resulting in turning angles of 11.9° ± 4.74° (P < 0.005) and 10.67°± 4.29° (P < 0.02), respectively (Fig. 6, B and C). Hsc70-depleted cortical neurons, however, were not attracted to the netrin-1 gradient in the chamber relative to the PBS controls, as the turning angle was reduced to −6.25° ± 3.03° (P > 0.07; Fig. 6, B and C). Importantly, exposure of neurons to the netrin-1 gradient did not significantly affect the displacement of the turning growth cones during the imaging period. However, the displacement of the Hsc70-depleted neurons was markedly reduced compared with the control siRNA or naive control neurons (Fig. 6 D). In fact, the mean displacement of all growth cones (including those excluded from turn calculations) of Hsc70-depleted neurons was fourfold reduced compared with control growth cones (Fig. 6, E and F). Furthermore, the proportion of growth cones that underwent temporal retraction or collapsed all together was much higher in Hsc70-depleted cortical growth cones (Fig. 6, G and H). These results demonstrate that Hsc70 is required for netrin-1–dependent attraction of cortical neurons in vitro and that Hsc70 supports axon extension dynamics.

Hsc70 chaperone activity is required for radial migration and callosal projections in the embryonic neocortex

Because the netrin-1/DCC signaling axis is important for corpus callosum formation (Izzi and Charron, 2011; Fothergill et al., 2014), we next examined the role of Hsc70 on netrin-1–dependent axonal projections in vivo. Embryonic telencephalons were transfected with pCIG2 vectors expressing GFP alone or GFP along with Hsc70 or $Hsc70^{D10N}$ by in utero electroporation at E14.5, when cortical progenitors exclusively generate upper layer commissural projection neurons (Langevin et al., 2007). After electroporation, embryos were left to develop for 3 d in utero before collection and processing. Coronal sections of E17.5 embryos were generated and GFP^+ commissural projections were assessed (Fig. 7 A). Whereas GFP^+ neurons expressing either the pCIG2 vector or Hsc70 all projected toward the corpus callosum as expected (n = 6 and 5 embryos, respectively; Fig. 7 A), callosal projections emanating from $Hsc70^{D10N}$-expressing neurons were impaired and failed to reach the corpus callosum (n = 11 embryos; Fig. 7 A, asterisk). This result is in agreement with studies showing that netrin-1 and DCC are required in vivo for corpus callosum formation (Serafini et al., 1996; Fazeli et al., 1997; Fothergill et al., 2014). Furthermore, the radial migration of $Hsc70^{D10N}$-expressing neurons toward the cortical plate was reduced (42.8 ± 11.2%) relative to pCIG2- or Hsc70-expressing neurons (68.17 ± 7.31% and 65.83 ± 14.84%, respectively; Fig. 7, A and B). Because neurons radially migrating through the intermediate zone are polarized by extending an apical or basal process (Kriegstein and Noctor, 2004), we next assessed the morphology of neurons expressing $Hsc70^{D10N}$ at higher magnification (Fig. 7, C and D). Within the intermediate zone, significantly more GFP^+ neurons expressing $Hsc70^{D10N}$ remained nonpolarized (32.6 ± 14.0% unpolarized $Hsc70^{D10N}$ neurons versus 5.23 ± 3.64% unpolarized control neurons; Fig. 7, C–E). Collectively, these results indicate that Hsc70 chaperone activity supports callosal projections and radial migration of neurons in vivo.

Discussion

Our data presented here outline a novel function for the molecular chaperone Hsc70 in regulating the Rac1 GEF Trio during netrin-1–mediated cortical axon growth and guidance (summarized in Fig. 8). We demonstrate that Hsc70 and Trio associate dynamically downstream of netrin-1 in cortical neurons and that the function of this association is dependent on Hsc70 chaperone activity. We support this finding with biochemical evidence highlighting that Hsc70 chaperone activity is required for Rac1 activation by Trio. Moreover, we correlate this function with the proper relocalization of Trio and cell surface DCC within cortical growth cones downstream of netrin-1. Hsc70 is a constitutive chaperone that is enriched in the developing CNS and constitutes 2–3% of total protein of the rat spinal cord (Aquino et al., 1993; Loones et al., 2000). Despite being 86% homologous to Hsp70, Hsc70 is preferentially ex-

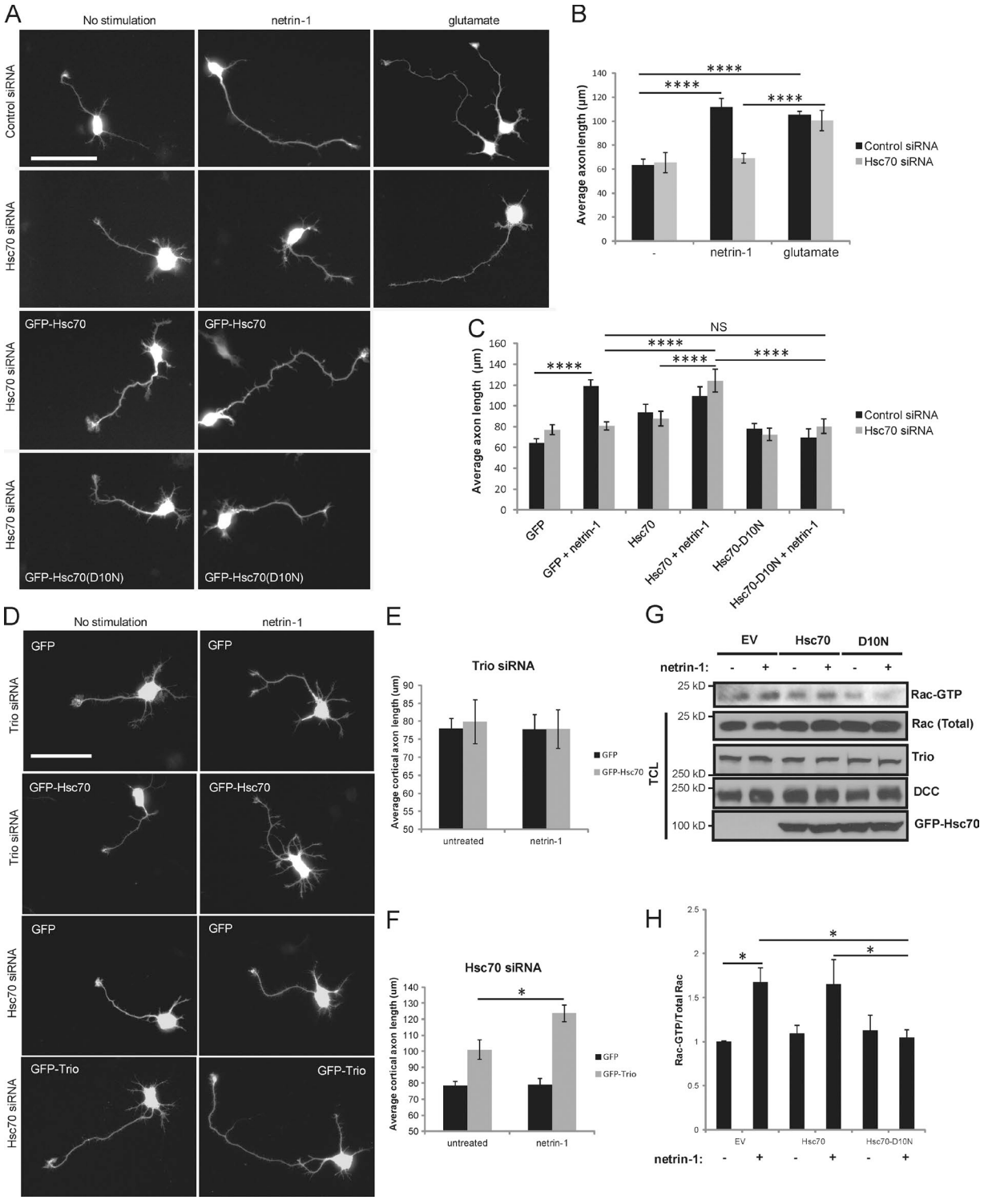

Figure 5. **Hsc70 is required for netrin-1–mediated cortical axon outgrowth and Rac1 activation.** (A) Dissociated E17.5 rat cortical neurons were electroporated with control siRNA or Hsc70 siRNA with a GFP reporter construct or the indicated GFP constructs. At DIV1, neurons were stimulated with netrin-1 or glutamate for 24 h. Bar, 50 µm. (B and C) The mean axon lengths of GFP+ neurons from A were calculated manually using Metamorph software (>50 neurons assessed per condition, from at least three independent experiments). Error bars indicate the SEM (****, $P < 0.0001$; one-way ANOVA, Fisher's least significant difference post-test). (D) E17.5 rat cortical neurons were depleted of endogenous Trio and Hsc70 by siRNA and reexpressed both with siRNA-resistant Hsc70 and Trio. (E and F) The mean axon lengths of GFP+ neurons were calculated as in B (>70 neurons assessed per condition, from at least three independent experiments). Error bars indicate the SEM (*, $P < 0.05$; unpaired *t* test). (G) HEK293 cells were transfected with pRK5-DCC with empty vector (EV), GFP-Hsc70, or GFP-Hsc70^{D10N} and stimulated with netrin-1 for 5 min. GTP-loaded Rac1 was pulled down from protein lysates by GST-CRIB. GTP-bound Rac1 (top), total Rac1, and the indicated proteins were detected by immunoblotting. TCL, total cell lysates. (H) Densitometric ratio of GTP-bound Rac1 to total Rac1 normalized to DCC. Error bars indicate the SEM ($n = 6$; *, $P < 0.05$; one-way ANOVA, Bonferroni's multiple comparisons test).

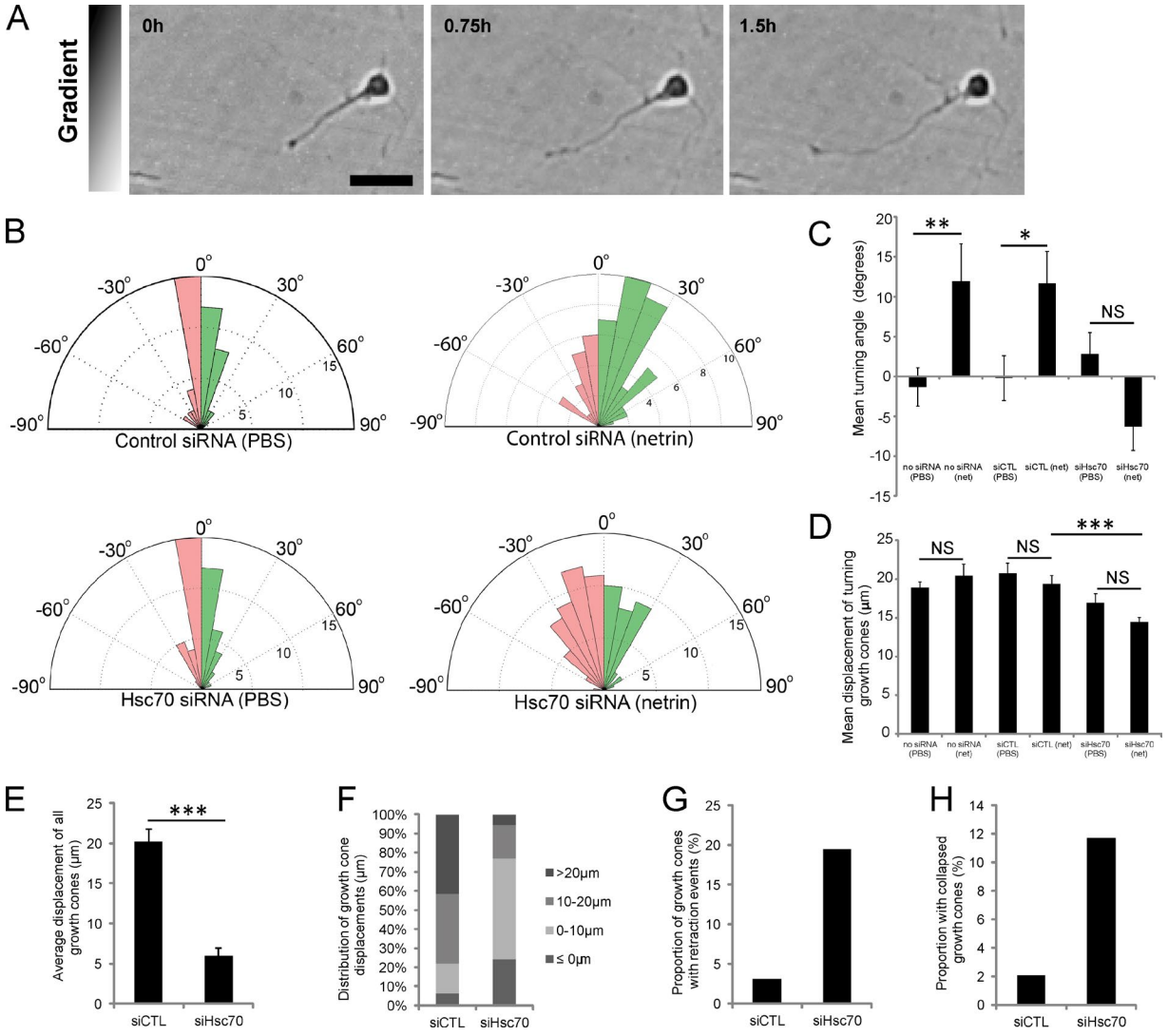

Figure 6. **Hsc70 is required for netrin-1–dependent attraction of embryonic cortical neurons.** Control (siCTL) or Hsc70 siRNA (siHsc70) was electroporated with a GFP reporter plasmid in E17.5 cortical neurons. At DIV2, neurons were exposed to vehicle PBS or a 200-ng/ml netrin-1 VI-V (net) gradient in Dunn chamber turning assays. (A) Video time-lapse imaging of control neurons exposed to a gradient for 90 min. Bar, 20 µm. (B) Rose histograms represent the distribution of turning angles of the cortical neurons. Green or pink indicate positive or negative turning angles, respectively. (C) Mean turning angles for each condition (>50 axons per condition, from at least three independent experiments). Error bars indicate the SEM (NS, $P > 0.05$; *, $P < 0.05$; **, $P < 0.01$; one-way ANOVA, Newman-Keuls multiple comparisons test). (D) The mean displacement of turning cortical growth cones over the 90-min imaging period. Error bars indicate the SEM ($n > 50$ axons per condition; NS, $P > 0.05$; ***, $P < 0.001$; one-way ANOVA, Newman-Keuls multiple comparisons test). (E) The mean displacement of all cortical growth cones over the 90-min imaging period (>70 axons per condition, from at least three independent experiments). Error bars indicate the SEM (***, $P < 0.001$; unpaired student's *t* test). (F) The distribution of growth cone displacements from E. (G) The proportion of growth cones from E with at least one retraction event. (H) The proportion of neurons from E with collapsed growth cones.

pressed in neurons whereas Hsp70 is enriched in glial cells in the unstressed mouse embryo (Loones et al., 2000). Hsc70 is an ATP-dependent chaperone that carries out various housekeeping chaperone functions; it assists in protein folding, translocation, chaperone-mediated autophagy, and prevention of protein aggregation (Daugaard et al., 2007).

Our study is the first to describe Hsc70-mediated regulation of a Rac1 GEF in neurons to date. In earlier studies, Hsc70 was reported to associate with other Rho GEFs including the protooncogenes Dbl and Plekhg4 (Kauppinen et al., 2005; Gupta et al., 2013). Similar to our findings for Trio, Kauppinen et al. (2005) demonstrated that the association of proto-Dbl with Hsc70 was mediated by the N terminus and Pleckstrin homology domain of the GEFD of proto-Dbl (Kauppinen et al., 2005). In direct contrast to our results, however, Hsc70 was identified as a negative regulator of proto-Dbl–induced RhoA GEF activity (Kauppinen et al., 2005). Although future studies are required to determine the precise mechanism of Hsc70-mediated regulation of Rho GEFs, our work highlights the exciting possibility that Hsc70 may serve as a universal regulator of Rho GEFs in specific cellular contexts. Elevated Hsc70 expression occurs in various tissues in which Rac1 is known to function, including in the neural tube during embryogenesis and in various types of cancer (Loones et al., 2000; Rohde et al., 2005; Duquette and Lamarche-Vane, 2014). Although Rac1 expression is elevated in primary tumors and Rac1 activation is required for cancer cell migration and metastasis (Bid et al., 2013), the dysregulation of Rac1 and Hsc70 has not yet been linked in any biological system. Currently, pharmacological inhibitors of Hsc70/Hsp70 are being tested as anti-cancer agents

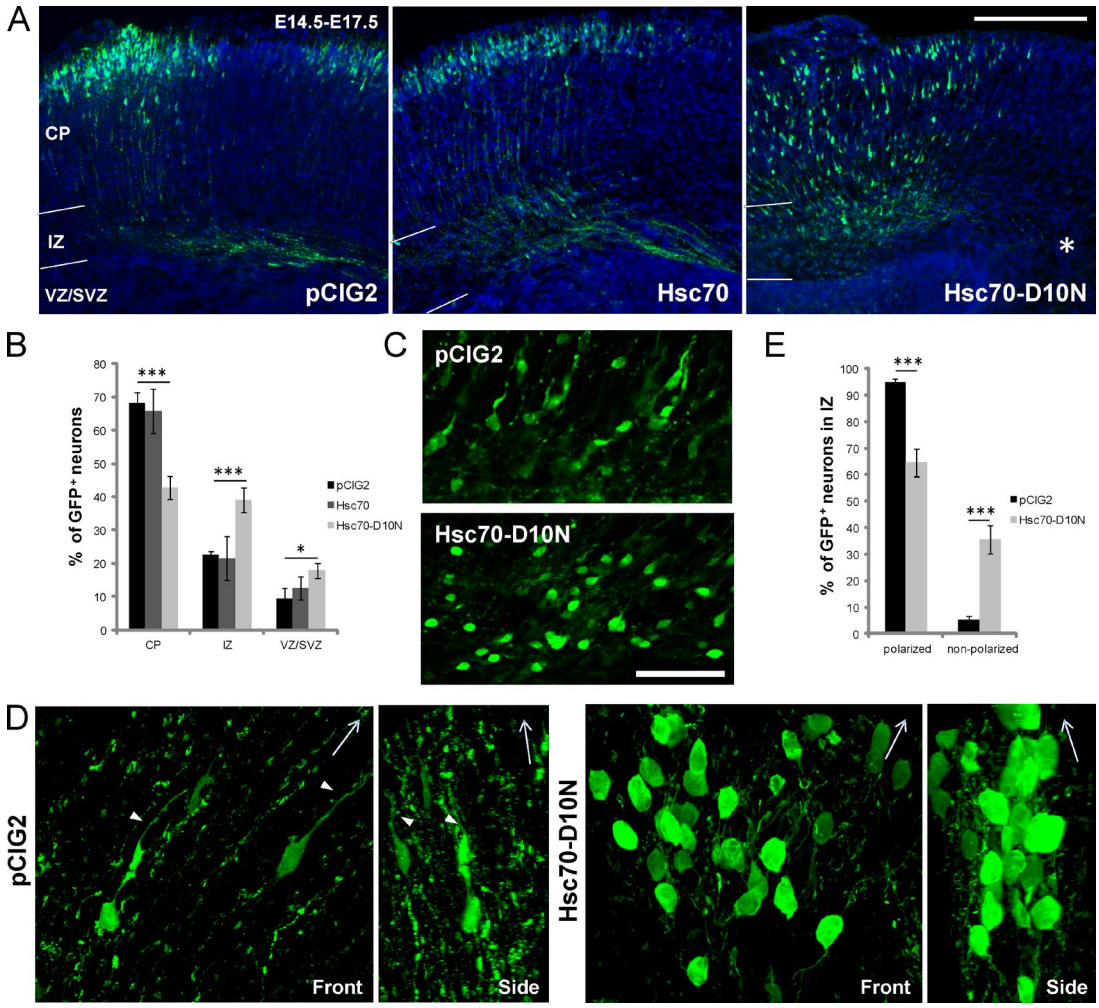

Figure 7. **Hsc70 chaperone activity supports radial neuronal migration and callosal projections in the embryonic neocortex.** (A) In utero electroporation of E14.5 mouse embryos with pCIG2 control vector or pCIG2 constructs encoding Hsc70 or Hsc70^{D10N}. Representative brightfield images of E17.5 coronal brain sections, stained with anti-GFP (green) and the nuclear marker DAPI (blue). Asterisk denotes impaired callosal projections. CP, cortical plate; IZ, intermediate zone; VZ/SVZ, ventricular zone/subventricular zone. Bar, 200 µm. (B) Quantification of the distribution of GFP$^+$ neurons in the cortex (pCIG2: 372 neurons from six embryos; Hsc70: 390 neurons from five embryos; Hsc70^{D10N}: 850 neurons from 11 embryos). Error bars indicate the SEM (*, $P < 0.05$; ***, $P < 0.001$; unpaired student's *t* test). (C) Morphological comparison of Hsc70^{D10N}-expressing neurons in the intermediate zone relative to vector control neurons. Bar, 50 µm. (D) High magnification 3D rendering of representative GFP$^+$ neurons in the intermediate zone from C revealing impaired neuronal polarization with Hsc70^{D10N} expression. Left, front view; right: side view. Arrows indicate direction of radial migration. Arrowheads indicate leading processes of migrating GFP$^+$ neurons. (E) Quantification of the proportion of GFP$^+$ neurons in the intermediate zone with polarized morphology (pCIG2: 288 neurons from seven embryos; Hsc70^{D10N}: 416 neurons from seven embryos). Error bars indicate the SEM (***, $P < 0.001$; unpaired student's *t* test).

and correlate with a function of Hsc70 in regulating Rac1-dependent processes such as cell proliferation and migration (Kaiser et al., 2011; Balaburski et al., 2013).

Furthermore, Rac1 signaling is required for neuronal polarization and migration during neocortex development (Azzarelli et al., 2015). Whereas wild-type Rac1 enhances neuronal migration, expression of dominant-negative or constitutively active Rac1 results in accumulation of neurons in the intermediate zone and failure to extend leading processes (Konno et al., 2005; Yang et al., 2012). Because Hsc70 is required for Trio-dependent Rac1 activation, the impeded polarization and radial migration of dominant-negative Hsc70^{D10N}-expressing neurons may be in part caused by dysregulation of Rac1. Normally, immature neurons go through a multipolar stage before becoming radially polarized during migration to the upper cortical layers (Nadarajah et al., 2001), thus the reduced polarization of Hsc70^{D10N}-expressing neurons is not a result of delayed neuronal differentiation. Further study should focus on whether this is because of Hsc70's function in regulating Rac1-dependent cytoskeletal dynamics or by a complementary component of cell migration. Indeed the endocytic machinery components clathrin and dynamin are also important for cortical neuron radial migration in vivo by supporting cell soma translocation (Shieh et al., 2011). Because Hsc70 is required for endocytosis and clathrin uncoating via dynamin regulation (Chang et al., 2002) it is likely that Hsc70 supports neuronal migration via both cytoskeletal and endosomal mechanisms.

Because the netrin-1–induced association of Hsc70 with DCC is prolonged in comparison to that with Trio alone, it suggests that Hsc70 may have an additional or downstream function in the DCC signaling complex independent of its regulation of Trio Rac1 GEF activity. The preferential association of Hsc70 with surface DCC further implies that Hsc70 in part regulates surface DCC localization or stability. Indeed we show

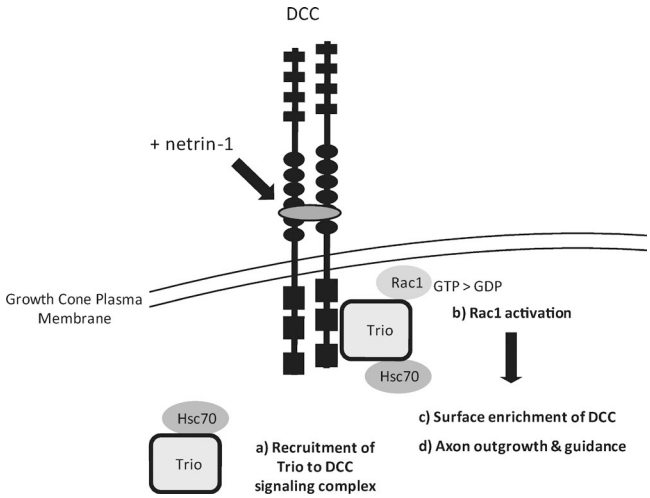

Figure 8. **Model of Trio regulation by Hsc70 during netrin-1/DCC signaling.** Netrin-1/DCC engagement results in recruitment of Trio and Hsc70 to DCC signaling complexes (a). Hsc70 chaperone activity is required for netrin-1–induced activation of Rac1 (b), surface DCC enrichment at the growth cone plasma membrane (c), and axon outgrowth and guidance downstream of netrin-1 (d). Therefore, we propose that Hsc70-mediated regulation of Trio is essential for the stability of the DCC/Trio signaling complex at the cell surface of growth cones to mediate netrin-1–induced cortical axon outgrowth and guidance.

that Hsc70 chaperone activity is required for the sustained enrichment of surface DCC in cortical growth cones downstream of netrin-1. Recruitment of DCC to the plasma membrane is important for netrin-1–induced axon guidance in cortical neurons. To date, a few mechanisms have been demonstrated that support netrin-1–induced DCC surface targeting from intracellular pools, including depolarization, activation of protein kinase A, and RhoA inhibition (Bouchard et al., 2004, 2008; Moore et al., 2008). We have previously reported that Trio supports the growth cone enrichment of surface DCC downstream of netrin-1 in cortical neurons (DeGeer et al., 2013). The Hsc70 ATPase activity is required for the stabilized enrichment of surface DCC at cortical growth cones treated with netrin-1. Therefore, we postulate that Hsc70 and Trio function by supporting the enrichment of surface DCC or permitting the mobilization of DCC from intracellular pools to the plasma membrane to allow a proper chemoattractive response of growth cones to netrin-1 (Fig. 8). Although further studies are required to delineate how Trio and Hsc70 contribute to surface DCC localization, one interesting possibility is local exocytosis of DCC-embedded vesicles. Previous studies report that netrin-1–induced axon outgrowth is dependent on exocytosis-driven plasma membrane insertion at the leading edge of the extending growth cone (Cotrufo et al., 2011; Winkle et al., 2014). Exocytosis and membrane fusion are mediated by the SNARE complex comprising a v-SNARE such as vesicle-associated membrane protein 2 and plasma membrane t-SNAREs, SNAP25 and syntaxin-1 (Südhof and Rothman, 2009). DCC forms a complex with syntaxin-1 downstream of netrin-1, and in this way it induces the local exocytosis of vesicle-associated membrane protein 2–expressing vesicles during axon outgrowth (Cotrufo et al., 2011). Furthermore, the E3 ubiquitin ligase TRIM9 associates directly with both SNAP-25 and DCC and promotes netrin-1–dependent axon branching in cortical neurons (Winkle et al., 2014). Interestingly, Hsc70 is closely linked to the exocytotic machinery at synapses by associating with vesicular cysteine-string protein α and SNAP25, enabling a SNARE complex formation at the plasma membrane (Sharma et al., 2011). In addition, another TRIM protein, TRIM22, has been recently connected to the Hsc70 partner C terminus of Hsc70-interacting protein (Gao et al., 2013), suggesting that Hsc70 may contribute in part to DCC-driven exocytosis through a TRIM9/SNAP25-dependent mechanism.

Although some evidence supports the ability for neurons to regenerate and form functional contacts after CNS injury, our knowledge of the cellular mechanisms underlying these processes and treatments for these conditions remains incomplete (Mar et al., 2014). Dysfunction of Hsc70 has been implicated in various neurodegenerative disorders including Huntington's, Parkinson's, and Alzheimer's diseases (Shimura et al., 2004; Koga et al., 2011; Turturici et al., 2011; Pemberton and Melki, 2012). To our knowledge this is the first study to implicate Hsc70 in the regulation of Rac1-dependent cellular processes, raising the possibility that Rac1 dysregulation in neurons contributes to the pathophysiology of neurodegenerative diseases (DeGeer and Lamarche-Vane, 2013). Indeed, Hsc70 expression is induced in response to cerebral ischemia, thus supporting a role for Hsc70 in axon regeneration and repair (Muranyi et al., 2005; Chen et al., 2007). It will be of great interest to investigate whether selectively augmenting Hsc70 chaperone activity will promote nerve regrowth in the context of neurodegeneration.

Materials and methods

DNA constructs, antibodies, and reagents

pEGFP-Trio and deletion mutants, pEGFP-Hsc70, pEGFP-Hsc70^{D10N}, pRK5-DCC, and pCIG2 constructs have been described previously (Estrach et al., 2002; Li et al., 2002; Hand et al., 2005; Briançon-Marjollet et al., 2008; Bański et al., 2010). Hsc70 and Hsc70^{D10N} cDNA were subcloned into the pCIG2 vector by PCR amplification using the forward primer (5′-CAGCGCTCGAGGCAACCATGTCTAAGGGACC-3′) and reverse primer (5′-CTTGAATTCTTAATCCACCTCTTCAATGG-3′) using standard cloning procedures. The rabbit polyclonal anti-TrioMTP antibody was generated by J. Boudeau (Centre de Recherche de Biochimie Macromoléculaire, Montpellier, France) as previously described using an antigen encompassing residues 1581–1849 of Trio-C isoform (DeGeer et al., 2013). Additional antibodies used were as follows: mouse anti-DCC$_{INT}$ (clone G97-449; BD), mouse anti-DCC$_{EXT}$ (clone AF5; EMD Millipore), rabbit anti-pERK1/2 (pThr202/pThr204) and anti-ERK1/2 (Cell Signaling Technology), rabbit anti-pFAK (pY861) and anti-FAK (Invitrogen), rabbit anti-GFP (Invitrogen), mouse anti-Hsc70 (clone B-6; Santa Cruz Biotechnology, Inc.), rabbit anti-Hsp70 (Enzo Life Sciences), mouse anti-Rac1 (BD), mouse anti-tubulin (EMD Millipore), and goat anti–rabbit Alexa Fluor 488 and goat anti–mouse Cy3 (Molecular Probes). Recombinant chick netrin-1 was secreted by 293-EBNA cells stably expressing chick netrin-1 (Serafini et al., 1994) tagged at its C terminus with the myc epitope and was purified by heparin affinity chromatography (GE Healthcare).

Cell culture and transfection

HEK293 cells were cultured at 37°C in DMEM (Wisent Bioproducts) supplemented with 10% FBS (Wisent Bioproducts), 2 mM L-glutamine, penicillin, and streptomycin (Invitrogen) under humidified conditions with 5% CO_2. Cells were transfected with the indicated constructs using linear polyethylenimine (PolySciences) at a 1:10 ratio (cDNA/polyethylenimine) as described previously (DeGeer et al., 2013).

Primary cortical neuron culture and electroporation

Cortical neurons from E17.5 rat embryos were dissociated mechanically and electroporated with cDNA constructs or siRNAs as indicated using the Amaxa Rat Neuron Nucleofector kit (Lonza). After electroporation, neurons were plated on either poly-D-lysine (0.1 mg/ml; Sigma-Aldrich)–coated dishes or poly-L-lysine (0.1 mg/ml, Sigma-Aldrich)–treated coverslips in 24-well plates at a density of 200,000 cells/well. Neurons were cultured in attachment medium (DMEM, 10% FBS, supplemented with 2 mM L-glutamine, penicillin, and streptomycin [Invitrogen]) under humidified conditions with 5% CO_2. After 1.5 h, the medium was replaced with maintenance medium (Neurobasal-A medium [Invitrogen], supplemented with 2% B27 [Invitrogen], 1% L-glutamine, penicillin, and streptomycin [Invitrogen]). After DIV1 or 2, the neurons were treated for the indicated times with recombinant netrin-1 (500 ng/ml). Down-regulation of endogenous Hsc70 was achieved by electroporating dissociated E17.5 rat cortical neurons with 150 nM synthetic Hsc70 siRNAs designed to target the 5′-UTR of the rat Hsc70 mRNA (5′-UCUGUGUGGUCUCGUCAUCUU-3′; Thermo Fisher Scientific) versus control siRNA (Silencer #1; Ambion) together with 4 µg of pmaxGFP vector (Lonza) used as a reporter. Only GFP-expressing neurons were assessed. The siRNA-resistant GFP-Hsc70 or GFP-Hsc70^{D10N} plasmids were coelectroporated where indicated, and expression of the exogenous proteins was verified by Western blotting (Fig. 2 H). Similarly, down-regulation of Trio was achieved by electroporating 300 nM of synthetic Trio siRNA (5′-GAACAUGAUUGACGAGCAUUU-3′; Thermo Fosher Scientific) as previously described (DeGeer et al., 2013).

Cortical tissue culture

Cortical tissues were extracted from E17.5 rat embryos. After light mechanical dissociation, tissues were transferred to a 4-well plate containing prewarmed maintenance medium and allowed to equilibrate to 37°C. Immediately after netrin-1 stimulation, samples were transferred to ice, collected, and processed as described previously (DeGeer et al., 2013).

Mass spectrometry analysis

E17.5 rat cortical tissue was treated with 500 ng/ml netrin-1 for 5 min, and protein lysates were collected and subsequently probed with anti-Trio antibodies conjugated to protein A–Sepharose beads. Antibody–protein complexes were resolved by SDS-PAGE, and proteins were visualized by silver staining. A prominent band of ∼65–75 kD was extracted from the gel and proteins were digested with trypsin and chymotrypsin. Peptide samples underwent mass spectrometric analysis (QTRAP4000 and MALDI-TOF, Genome Innovation Centre, Montreal, Canada). Mascot searches of resulting sequences were performed using the UniProt database with a rat filter and identified five peptides corresponding to Hsc70.

Immunoprecipitation and immunoblotting

Cortical tissues were lysed in buffer containing 20 mM Hepes, pH 7.5, 100 mM NaCl, 10% glycerol, 1% Triton X-100, 20 mM sodium fluoride, 1 mM sodium orthovanadate, 1 mM PMSF, and 1 µg/ml aprotinin and leupeptin (BioShop). Protein lysates were centrifuged at 10,000 *g* for 5 min at 4°C to remove insoluble materials. For immunoprecipitation from primary cortical lysates, 1 mg of protein lysate underwent preclearing with protein A– or G–Sepharose beads for 1 h at 4°C. Supernatants were then incubated for 1 h at 4°C with 9 µg of rabbit anti-TrioMTP or 1.5 µg of mouse anti-DCC (AF-5) followed by addition of 40 µl of protein A– or G–Sepharose beads for 2 h (GE Healthcare). Beads were washed a minimum of four times with ice-cold lysis buffer and heated to 95°C in SDS sample buffer. Protein samples were resolved by SDS-PAGE, transferred to nitrocellulose membranes for immunoblotting with the appropriate antibodies, and visualized by ECL (PerkinElmer). For surface and intracellular DCC immunoprecipitations, cortical neurons were treated with or without 500 ng/ml of netrin-1 for 5 min and transferred to ice. Cells were then washed with ice-cold PBS containing 1 mM magnesium chloride and 0.1 mM calcium chloride and then blocked in ice-cold 1% BSA/PBS for 20 min. After blocking, the cells were incubated with either mouse IgGs or mouse anti-DCC_{EXT} (AF-5) antibodies at 1 µg/ml in ice-cold PBS for 40 min on ice, followed by three, 5-min washes with cold PBS. Proteins were extracted with RIPA buffer (150 mM NaCl, 50 mM Hepes, pH 7.5, 1% NP-40, 10 mM EDTA, pH 8.0, 0.5% sodium deoxycholate, 0.1% SDS, 20 mM sodium fluoride, 1 mM sodium orthovanadate, 1 mM PMSF, and 1 µg/ml aprotinin and leupeptin [BioShop]), and protein lysates were centrifuged at 10,000 *g* for 5 min at 4°C. Surface DCC was isolated by incubation with protein G–Sepharose beads for 1 h at 4°C. The supernatant corresponding to the intracellular DCC pool was collected for each sample, and immunoprecipitations were subsequently performed with either IgGs or anti-DCC.

Rac1 activation assay

Transfected HEK293 cells were serum starved overnight and then lysed in buffer containing 25 mM Hepes, pH 7.5, 1% NP-40, 10 mM $MgCl_2$, 100 mM NaCl, 5% glycerol, 1 mM PMSF, and 1 µg/ml aprotinin and leupeptin (BioShop). Protein lysates were centrifuged at 10,000 *g* for 2 min at 4°C to remove insoluble materials. Endogenous GTP-Rac1 was pulled down by incubating the protein lysates for 30 min at 4°C with the CRIB domain of mouse PAK3 (amino acids 73–146) fused to GST and coupled to glutathione-Sepharose beads. The beads were washed twice with 25 mM Hepes, pH 7.5, 1% NP-40, 30 mM $MgCl_2$, 40 mM NaCl, and 1 mM DTT and resuspended in SDS sample buffer. Protein samples were resolved by SDS-PAGE and transferred onto nitrocellulose membranes for immunoblotting with the anti-Rac1 antibody. The levels of GTP-bound Rac1 were assessed by densitometry using Quantity One software (Bio-Rad Laboratories) and normalized to the total amount of GTPases detected in the total cell lysates.

Immunofluorescence, microscopy, and Pearson's correlation coefficient

Cortical neurons (DIV1 or 2) were fixed with 3.7% formaldehyde (Sigma-Aldrich) in 20% sucrose/PBS for 30 min at 37°C and permeabilized as described previously (DeGeer et al., 2013). Immunostaining was performed with the indicated primary antibodies and the respective Cy3 or Alexa Fluor 488–conjugated secondary antibodies and all coverslips were mounted with ProLong Gold Antifade reagent (Invitrogen). To assess protein colocalization, coimmunostained cortical neurons were imaged on a laser-scanning confocal microscope (LSM510; Carl Zeiss) with a Plan Apochromat 63×/1.4 oil immersion objective lens and analyzed with Zen2009 software (Carl Zeiss). Quantification of colocalization using Pearson's correlation coefficient was performed using MetaMorph software (Molecular Devices), analyzing >15 neurons per condition in at least three independent experiments. One-way analysis of variance (ANOVA) was performed, and the data were presented as a mean $r \pm$ SEM. For axon outgrowth assays, neurons were visualized with a motorized inverted microscope (IX81; Olympus) using a 40× U Pplan Fluorite oil immersion objective lens. Images were recorded with a CoolSnap 4K camera (Photometrics) and analyzed with Metamorph software. For surface DCC detection, cortical neurons remained unpermeabilized, were blocked in 1% BSA/PBS, and were incubated with anti-DCC_{EXT} in 1% BSA/PBS at 4°C overnight. Cy3-conjugated secondary antibodies were used to label surface DCC. Images were acquired as for the axon outgrowth experiments, and the mean pixel intensity of DCC fluorescence on growth cones and axonal surfaces was measured from acquired images using Metamorph software, using exclusive thresholding to eliminate background fluorescence.

Axon outgrowth analysis and Dunn chamber assays

To analyze axon outgrowth of primary cortical neurons (DIV2), electroporated (GFP^+) cells were analyzed for each condition from at least three independent experiments. Axon lengths were measured manually from acquired images with MetaMorph software. One-way ANOVA with Fisher's least significant difference post-test was used for statistical analysis, and the data were presented as the mean cortical neuron axon length ± SEM. For turning assays, dissociated cortical neurons (DIV2) were plated on coverslips used for Dunn chamber assembly as previously described (Yam et al., 2009). Gradients were generated with purified netrin-1 VI-V (200 ng/ml) or buffer containing PBS in the outer well. Cell images were acquired every 3–4 min for at least 90 min at 37°C on a temperature controlled stage. Neurites of at least 10-µm length were tracked in GFP-expressing neurons. The final position of the growth cone was used to determine the angle turned over 90 min relative to the gradient position. Measurements are presented in rose histograms in bins of 10° with the length of each segment representing the frequency of measurements in percent. Mean turning angle and mean displacement are also represented.

In utero electroporation

CD1 mouse embryos were staged using the morning of the vaginal plug as E0.5. To drive GFP reporter expression in layer II/III neurons, E14.5 embryos were electroporated with pCIG2 expression vectors containing an IRES-EGFP cassette under the control of the CAG promoter (Hand et al., 2005). In utero electroporation was performed essentially as described previously (Langevin et al., 2007). In brief, 3 µg/µl of plasmid was injected into the telencephalon and electroporated using 6× 50-V/50-ms square wave pulses with 1-s intervals.

Histology

Immunohistochemistry was performed as previously described (Langevin et al., 2007). In brief, dissected E17.5 brains were fixed overnight at 4°C in 4% paraformaldehyde/PBS. Brains were cryoprotected in 20% sucrose/PBS at 4°C overnight and frozen in OCT on liquid nitrogen. Cryosections (16 µm) were collected on Superfrost Plus slides (Thermo Fisher Scientific). Blocking and antibody incubations (anti-GFP, 1:1,000) were performed in PBS supplemented with 0.4% Triton X-100 and 0.3% BSA, and all washes were with PBS. Slides were mounted in Mowiol (EMD Millipore) and imaging was performed using an Imager M2 upright microscope (Carl Zeiss) with an AxioCam ICc5 camera (Carl Zeiss) or a laser-scanning confocal microscope (LSM780; Carl Zeiss) with a Plan Apochromat 20×/0.8 or 63×/1.4 oil differential interference contrast objective lenses. Images were processed with Zen software and Photoshop CS5 (Adobe). Cortical layers were subdivided based on cell density, and neuronal migration was scored from confocal images (>350 GFP^+ neurons from at least five brains, per condition). Neuronal polarization of GFP^+ cells in the intermediate zone were scored by assessing maximal projections of confocal Z-stacks taken at 0.5-µm increments to visualize processes out of plane (>250 GFP^+ neurons from at least six brains, per condition). Nonpolarized neurons were considered round cells without any processes.

Statistical analysis

Statistical analysis was performed with GraphPad Prism 6 (GraphPad Software). The data are presented as the mean ± the SEM.

Acknowledgments

We are grateful to Jérôme Boudeau for the anti-Trio antibodies. We thank Min Fu and the imaging core facility of the Research Institute of the McGill University Health Centre for assistance with confocal microscopy. We thank Heena Kumra and Dieter Reinhardt for assistance with brightfield microscopy. We also thank Line Roy and Daniel Boismenu for their assistance with the mass spectrometry analysis.

This research was supported by the Canadian Institute of Health Research grant MOP-14701 (to N. Lamarche-Vane) and MOP-102584 (to M. Cayouette) and the Canada Foundation for Innovation-Leaders Opportunity Fund to N. Lamarche-Vane. N. Lamarche-Vane was a recipient of a Fonds de la Recherche en Santé du Québec Chercheur-National and a William Dawson Scholar.

The authors declare no competing financial interests.

Submitted: 19 May 2015
Accepted: 21 July 2015

References

Ackerman, S.L., L.P. Kozak, S.A. Przyborski, L.A. Rund, B.B. Boyer, and B.B. Knowles. 1997. The mouse rostral cerebellar malformation gene encodes an UNC-5-like protein. *Nature.* 386:838–842. http://dx.doi.org/10.1038/386838a0

Antoine-Bertrand, J., J.F. Villemure, and N. Lamarche-Vane. 2011. Implication of rho GTPases in neurodegenerative diseases. *Curr. Drug Targets.* 12:1202–1215. http://dx.doi.org/10.2174/138945011795906543

Aquino, D.A., A.A. Klipfel, C.F. Brosnan, and W.T. Norton. 1993. The 70-kDa heat shock cognate protein (HSC70) is a major constituent of the central nervous system and is up-regulated only at the mRNA level in acute experimental autoimmune encephalomyelitis. *J. Neurochem.* 61:1340–1348. http://dx.doi.org/10.1111/j.1471-4159.1993.tb13627.x

Azzarelli, R., T. Kerloch, and E. Pacary. 2015. Regulation of cerebral cortex development by Rho GTPases: insights from *in vivo* studies. *Front. Cell. Neurosci.* 8:445.

Balaburski, G.M., J.I. Leu, N. Beeharry, S. Hayik, M.D. Andrake, G. Zhang, M. Herlyn, J. Villanueva, R.L.J. Dunbrack Jr., T. Yen, et al. 2013. A modified HSP70 inhibitor shows broad activity as an anticancer agent. *Mol. Cancer Res.* 11:219–229. http://dx.doi.org/10.1158/1541-7786.MCR-12-0547-T

Bański, P., H. Mahboubi, M. Kodiha, S. Shrivastava, C. Kanagaratham, and U. Stochaj. 2010. Nucleolar targeting of the chaperone hsc70 is regulated by stress, cell signaling, and a composite targeting signal which is controlled by autoinhibition. *J. Biol. Chem.* 285:21858–21867. http://dx.doi.org/10.1074/jbc.M110.117291

Barallobre, M.J., M. Pascual, J.A. Del Río, and E. Soriano. 2005. The Netrin family of guidance factors: emphasis on Netrin-1 signalling. *Brain Res. Brain Res. Rev.* 49:22–47. http://dx.doi.org/10.1016/j.brainresrev.2004.11.003

Bashaw, G.J., and R. Klein. 2010. Signaling from axon guidance receptors. *Cold Spring Harb. Perspect. Biol.* 2:a001941. http://dx.doi.org/10.1101/cshperspect.a001941

Bellanger, J.-M., J.B. Lazaro, S. Diriong, A. Fernandez, N. Lamb, and A. Debant. 1998. The two guanine nucleotide exchange factor domains of Trio link the Rac1 and the RhoA pathways in vivo. *Oncogene.* 16:147–152. http://dx.doi.org/10.1038/sj.onc.1201532

Bid, H.K., R.D. Roberts, P.K. Manchanda, and P.J. Houghton. 2013. RAC1: an emerging therapeutic option for targeting cancer angiogenesis and metastasis. *Mol. Cancer Ther.* 12:1925–1934. http://dx.doi.org/10.1158/1535-7163.MCT-13-0164

Blangy, A., E. Vignal, S. Schmidt, A. Debant, C. Gauthier-Rouvière, and P. Fort. 2000. TrioGEF1 controls Rac- and Cdc42-dependent cell structures through the direct activation of rhoG. *J. Cell Sci.* 113:729–739.

Bouchard, J.-F., S.W. Moore, N.X. Tritsch, P.P. Roux, M. Shekarabi, P.A. Barker, and T.E. Kennedy. 2004. Protein kinase A activation promotes plasma membrane insertion of DCC from an intracellular pool: a novel mechanism regulating commissural axon extension. *J. Neurosci.* 24:3040–3050. http://dx.doi.org/10.1523/JNEUROSCI.4934-03.2004

Bouchard, J.-F., K.E. Horn, T. Stroh, and T.E. Kennedy. 2008. Depolarization recruits DCC to the plasma membrane of embryonic cortical neurons and enhances axon extension in response to netrin-1. *J. Neurochem.* 107:398–417. http://dx.doi.org/10.1111/j.1471-4159.2008.05609.x

Briançon-Marjollet, A., A. Ghogha, H. Nawabi, I. Triki, C. Auziol, S. Fromont, C. Piché, H. Enslen, K. Chebli, J.F. Cloutier, et al. 2008. Trio mediates

netrin-1-induced Rac1 activation in axon outgrowth and guidance. *Mol. Cell. Biol.* 28:2314–2323. http://dx.doi.org/10.1128/MCB.00998-07

Chang, H.C., S.L. Newmyer, M.J. Hull, M. Ebersold, S.L. Schmid, and I. Mellman. 2002. Hsc70 is required for endocytosis and clathrin function in *Drosophila*. *J. Cell Biol.* 159:477–487. http://dx.doi.org/10.1083/jcb.200205086

Chen, A., W.P. Liao, Q. Lu, W.S. Wong, and P.T. Wong. 2007. Upregulation of dihydropyrimidinase-related protein 2, spectrin α II chain, heat shock cognate protein 70 pseudogene 1 and tropomodulin 2 after focal cerebral ischemia in rats—a proteomics approach. *Neurochem. Int.* 50:1078–1086. http://dx.doi.org/10.1016/j.neuint.2006.11.008

Cook, D.R., K.L. Rossman, and C.J. Der. 2014. Rho guanine nucleotide exchange factors: regulators of Rho GTPase activity in development and disease. *Oncogene.* 33:4021–4035. http://dx.doi.org/10.1038/onc.2013.362

Cotrufo, T., F. Pérez-Brangulí, A. Muhaisen, O. Ros, R. Andrés, T. Baeriswyl, G. Fuschini, T. Tarrago, M. Pascual, J. Ureña, et al. 2011. A signaling mechanism coupling netrin-1/deleted in colorectal cancer chemoattraction to SNARE-mediated exocytosis in axonal growth cones. *J. Neurosci.* 31:14463–14480. http://dx.doi.org/10.1523/JNEUROSCI.3018-11.2011

Daugaard, M., M. Rohde, and M. Jäättelä. 2007. The heat shock protein 70 family: Highly homologous proteins with overlapping and distinct functions. *FEBS Lett.* 581:3702–3710. http://dx.doi.org/10.1016/j.febslet.2007.05.039

Debant, A., C. Serra-Pagès, K. Seipel, S. O'Brien, M. Tang, S.H. Park, and M. Streuli. 1996. The multidomain protein Trio binds the LAR transmembrane tyrosine phosphatase, contains a protein kinase domain, and has separate rac-specific and rho-specific guanine nucleotide exchange factor domains. *Proc. Natl. Acad. Sci. USA.* 93:5466–5471. http://dx.doi.org/10.1073/pnas.93.11.5466

DeGeer, J., and N. Lamarche-Vane. 2013. Rho GTPases in neurodegeneration diseases. *Exp. Cell Res.* 319:2384–2394. http://dx.doi.org/10.1016/j.yexcr.2013.06.016

DeGeer, J., J. Boudeau, S. Schmidt, F. Bedford, N. Lamarche-Vane, and A. Debant. 2013. Tyrosine phosphorylation of the Rho guanine nucleotide exchange factor Trio regulates netrin-1/DCC-mediated cortical axon outgrowth. *Mol. Cell. Biol.* 33:739–751. http://dx.doi.org/10.1128/MCB.01264-12

Duquette, P.M., and N. Lamarche-Vane. 2014. Rho GTPases in embryonic development. *Small GTPases.* 5:8. http://dx.doi.org/10.4161/sgtp.29716

Estrach, S., S. Schmidt, S. Diriong, A. Penna, A. Blangy, P. Fort, and A. Debant. 2002. The human Rho-GEF trio and its target GTPase RhoG are involved in the NGF pathway, leading to neurite outgrowth. *Curr. Biol.* 12:307–312. http://dx.doi.org/10.1016/S0960-9822(02)00658-9

Fazeli, A., S.L. Dickinson, M.L. Hermiston, R.V. Tighe, R.G. Steen, C.G. Small, E.T. Stoeckli, K. Keino-Masu, M. Masu, H. Rayburn, et al. 1997. Phenotype of mice lacking functional *Deleted in colorectal cancer* (*Dcc*) gene. *Nature.* 386:796–804. http://dx.doi.org/10.1038/386796a0

Fothergill, T., A.L. Donahoo, A. Douglass, O. Zalucki, J. Yuan, T. Shu, G.J. Goodhill, and L.J. Richards. 2014. Netrin-DCC signaling regulates corpus callosum formation through attraction of pioneering axons and by modulating Slit2-mediated repulsion. *Cereb. Cortex.* 24:1138–1151. http://dx.doi.org/10.1093/cercor/bhs395

Gao, B., Y. Wang, W. Xu, S. Li, Q. Li, and S. Xiong. 2013. Inhibition of histone deacetylase activity suppresses IFN-γ induction of tripartite motif 22 via CHIP-mediated proteasomal degradation of IRF-1. *J. Immunol.* 191:464–471. http://dx.doi.org/10.4049/jimmunol.1203533

Grant, A., F. Fathalli, G. Rouleau, R. Joober, and C. Flores. 2012. Association between schizophrenia and genetic variation in *DCC*: a case–control study. *Schizophr. Res.* 137:26–31. http://dx.doi.org/10.1016/j.schres.2012.02.023

Guan, K.L., and Y. Rao. 2003. Signalling mechanisms mediating neuronal responses to guidance cues. *Nat. Rev. Neurosci.* 4:941–956. http://dx.doi.org/10.1038/nrn1254

Gupta, M., E. Kamynina, S. Morley, S. Chung, N. Muakkassa, H. Wang, S. Brathwaite, G. Sharma, and D. Manor. 2013. Plekhg4 is a novel Dbl family guanine nucleotide exchange factor protein for rho family GTPases. *J. Biol. Chem.* 288:14522–14530. http://dx.doi.org/10.1074/jbc.M112.430371

Hand, R., D. Bortone, P. Mattar, L. Nguyen, J.I. Heng, S. Guerrier, E. Boutt, E. Peters, A.P. Barnes, C. Parras, et al. 2005. Phosphorylation of Neurogenin2 specifies the migration properties and the dendritic morphology of pyramidal neurons in the neocortex. *Neuron.* 48:45–62. http://dx.doi.org/10.1016/j.neuron.2005.08.032

Hartl, F.U., A. Bracher, and M. Hayer-Hartl. 2011. Molecular chaperones in protein folding and proteostasis. *Nature.* 475:324–332. http://dx.doi.org/10.1038/nature10317

Huber, A.B., A.L. Kolodkin, D.D. Ginty, and J.F. Cloutier. 2003. Signaling at the growth cone: ligand-receptor complexes and the control of axon growth and guidance. *Annu. Rev. Neurosci.* 26:509–563. http://dx.doi.org/10.1146/annurev.neuro.26.010302.081139

Izzi, L., and F. Charron. 2011. Midline axon guidance and human genetic disorders. *Clin. Genet.* 80:226–234. http://dx.doi.org/10.1111/j.1399-0004.2011.01735.x

Jaffe, A.B., and A. Hall. 2005. Rho GTPases: biochemistry and biology. *Annu. Rev. Cell Dev. Biol.* 21:247–269. http://dx.doi.org/10.1146/annurev.cellbio.21.020604.150721

Kaiser, M., A. Kühnl, J. Reins, S. Fischer, J. Ortiz-Tanchez, C. Schlee, L.H. Mochmann, S. Heesch, O. Benlasfer, W.-K. Hofmann, et al. 2011. Antileukemic activity of the HSP70 inhibitor pifithrin-μ in acute leukemia. *Blood Cancer J.* 1:e28. http://dx.doi.org/10.1038/bcj.2011.28

Kauppinen, K.P., F. Duan, J.I. Wels, and D. Manor. 2005. Regulation of the Dbl proto-oncogene by heat shock cognate protein 70 (Hsc70). *J. Biol. Chem.* 280:21638–21644. http://dx.doi.org/10.1074/jbc.M413984200

Keino-Masu, K., M. Masu, L. Hinck, E.D. Leonardo, S.S.-Y. Chan, J.G. Culotti, and M. Tessier-Lavigne. 1996. Deleted in Colorectal Cancer (DCC) encodes a netrin receptor. *Cell.* 87:175–185. http://dx.doi.org/10.1016/S0092-8674(00)81336-7

Kennedy, T.E., T. Serafini, J.R. de la Torre, and M. Tessier-Lavigne. 1994. Netrins are diffusible chemotropic factors for commissural axons in the embryonic spinal cord. *Cell.* 78:425–435. http://dx.doi.org/10.1016/0092-8674(94)90421-9

Kim, T.H., H.K. Lee, I.A. Seo, H.R. Bae, D.J. Suh, J. Wu, Y. Rao, K.G. Hwang, and H.T. Park. 2005. Netrin induces down-regulation of its receptor, Deleted in Colorectal Cancer, through the ubiquitin–proteasome pathway in the embryonic cortical neuron. *J. Neurochem.* 95:1–8. http://dx.doi.org/10.1111/j.1471-4159.2005.03314.x

Koga, H., M. Martinez-Vicente, E. Arias, S. Kaushik, D. Sulzer, and A.M. Cuervo. 2011. Constitutive upregulation of chaperone-mediated autophagy in Huntington's disease. *J. Neurosci.* 31:18492–18505. http://dx.doi.org/10.1523/JNEUROSCI.3219-11.2011

Konno, D., S. Yoshimura, K. Hori, H. Maruoka, and K. Sobue. 2005. Involvement of the phosphatidylinositol 3-kinase/rac1 and cdc42 pathways in radial migration of cortical neurons. *J. Biol. Chem.* 280:5082–5088. http://dx.doi.org/10.1074/jbc.M408251200

Kriegstein, A.R., and S.C. Noctor. 2004. Patterns of neuronal migration in the embryonic cortex. *Trends Neurosci.* 27:392–399. http://dx.doi.org/10.1016/j.tins.2004.05.001

Langevin, L.M., P. Mattar, R. Scardigli, M. Roussigné, C. Logan, P. Blader, and C. Schuurmans. 2007. Validating in utero electroporation for the rapid analysis of gene regulatory elements in the murine telencephalon. *Dev. Dyn.* 236:1273–1286. http://dx.doi.org/10.1002/dvdy.21126

Laurin, M., and J.F. Côté. 2014. Insights into the biological functions of Dock family guanine nucleotide exchange factors. *Genes Dev.* 28:533–547. http://dx.doi.org/10.1101/gad.236349.113

Leonardo, E.D., L. Hinck, M. Masu, K. Keino-Masu, S.L. Ackerman, and M. Tessier-Lavigne. 1997. Vertebrate homologues of *C. elegans* UNC-5 are candidate netrin receptors. *Nature.* 386:833–838. http://dx.doi.org/10.1038/386833a0

Lesnick, T.G., E.J. Sorenson, J.E. Ahlskog, J.R. Henley, L. Shehadeh, S. Papapetropoulos, and D.M. Maraganore. 2008. Beyond Parkinson disease: amyotrophic lateral sclerosis and the axon guidance pathway. *PLoS ONE.* 3:e1449. http://dx.doi.org/10.1371/journal.pone.0001449

Li, X., E. Saint-Cyr-Proulx, K. Aktories, and N. Lamarche-Vane. 2002. Rac1 and Cdc42 but not RhoA or Rho kinase activities are required for neurite outgrowth induced by the Netrin-1 receptor DCC (deleted in colorectal cancer) in N1E-115 neuroblastoma cells. *J. Biol. Chem.* 277:15207–15214. http://dx.doi.org/10.1074/jbc.M109913200

Li, W., J. Lee, H.G. Vikis, S.H. Lee, G. Liu, J. Aurandt, T.L. Shen, E.R. Fearon, J.L. Guan, M. Han, et al. 2004. Activation of FAK and Src are receptor-proximal events required for netrin signaling. *Nat. Neurosci.* 7:1213–1221. http://dx.doi.org/10.1038/nn1329

Li, X., X. Gao, G. Liu, W. Xiong, J. Wu, and Y. Rao. 2008. Netrin signal transduction and the guanine nucleotide exchange factor DOCK180 in attractive signaling. *Nat. Neurosci.* 11:28–35. http://dx.doi.org/10.1038/nn2022

Lin, L., T.G. Lesnick, D.M. Maraganore, and O. Isacson. 2009. Axon guidance and synaptic maintenance: preclinical markers for neurodegenerative disease and therapeutics. *Trends Neurosci.* 32:142–149. http://dx.doi.org/10.1016/j.tins.2008.11.006

Liu, G., H. Beggs, C. Jürgensen, H.T. Park, H. Tang, J. Gorski, K.R. Jones, L.F. Reichardt, J. Wu, and Y. Rao. 2004. Netrin requires focal adhesion kinase and Src family kinases for axon outgrowth and attraction. *Nat. Neurosci.* 7:1222–1232. http://dx.doi.org/10.1038/nn1331

Liu, G., W. Li, L. Wang, A. Kar, K.L. Guan, Y. Rao, and J.Y. Wu. 2009. DSCAM functions as a netrin receptor in commissural axon pathfinding. *Proc. Natl. Acad. Sci. USA.* 106:2951–2956. http://dx.doi.org/10.1073/pnas.0811083106

Loones, M.T., Y. Chang, and M. Morange. 2000. The distribution of heat shock proteins in the nervous system of the unstressed mouse embryo suggests a role in neuronal and non-neuronal differentiation. *Cell Stress Chaperones.* 5:291–305. http://dx.doi.org/10.1379/1466-1268(2000)005<0291:TDOHSP>2.0.CO;2

Lowery, L.A., and D. Van Vactor. 2009. The trip of the tip: understanding the growth cone machinery. *Nat. Rev. Mol. Cell Biol.* 10:332–343. http://dx.doi.org/10.1038/nrm2679

Ly, A., A. Nikolaev, G. Suresh, Y. Zheng, M. Tessier-Lavigne, and E. Stein. 2008. DSCAM is a netrin receptor that collaborates with DCC in mediating turning responses to netrin-1. *Cell.* 133:1241–1254. http://dx.doi.org/10.1016/j.cell.2008.05.030

Mar, F.M., A. Bonni, and M.M. Sousa. 2014. Cell intrinsic control of axon regeneration. *EMBO Rep.* 15:254–263. http://dx.doi.org/10.1002/embr.201337723

Meriane, M., J. Tcherkezian, C.A. Webber, E.I. Danek, I. Triki, S. McFarlane, E. Bloch-Gallego, and N. Lamarche-Vane. 2004. Phosphorylation of DCC by Fyn mediates Netrin-1 signaling in growth cone guidance. *J. Cell Biol.* 167:687–698. http://dx.doi.org/10.1083/jcb.200405053

Moore, S.W., J.P. Correia, K. Lai Wing Sun, M. Pool, A.E. Fournier, and T.E. Kennedy. 2008. Rho inhibition recruits DCC to the neuronal plasma membrane and enhances axon chemoattraction to netrin 1. *Development.* 135:2855–2864. http://dx.doi.org/10.1242/dev.024133

Muranyi, M., Q.P. He, K.S. Fong, and P.A. Li. 2005. Induction of heat shock proteins by hyperglycemic cerebral ischemia. *Brain Res. Mol. Brain Res.* 139:80–87. http://dx.doi.org/10.1016/j.molbrainres.2005.05.023

Nadarajah, B., J.E. Brunstrom, J. Grutzendler, R.O. Wong, and A.L. Pearlman. 2001. Two modes of radial migration in early development of the cerebral cortex. *Nat. Neurosci.* 4:143–150. http://dx.doi.org/10.1038/83967

O'Brien, S.P., K. Seipel, Q.G. Medley, R. Bronson, R. Segal, and M. Streuli. 2000. Skeletal muscle deformity and neuronal disorder in Trio exchange factor-deficient mouse embryos. *Proc. Natl. Acad. Sci. USA.* 97:12074–12078. http://dx.doi.org/10.1073/pnas.97.22.12074

Olofsson, B. 1999. Rho guanine dissociation inhibitors: pivotal molecules in cellular signalling. *Cell. Signal.* 11:545–554. http://dx.doi.org/10.1016/S0898-6568(98)00063-1

Pemberton, S., and R. Melki. 2012. The interaction of Hsc70 protein with fibrillar α-Synuclein and its therapeutic potential in Parkinson's disease. *Commun. Integr. Biol.* 5:94–95. http://dx.doi.org/10.4161/cib.18483

Picard, M., R.J. Petrie, J. Antoine-Bertrand, E. Saint-Cyr-Proulx, J.F. Villemure, and N. Lamarche-Vane. 2009. Spatial and temporal activation of the small GTPases RhoA and Rac1 by the netrin-1 receptor UNC5a during neurite outgrowth. *Cell. Signal.* 21:1961–1973. http://dx.doi.org/10.1016/j.cellsig.2009.09.004

Portales-Casamar, E., A. Briançon-Marjollet, S. Fromont, R. Triboulet, and A. Debant. 2006. Identification of novel neuronal isoforms of the Rho-GEF Trio. *Biol. Cell.* 98:183–193. http://dx.doi.org/10.1042/BC20050009

Rama, N., D. Goldschneider, V. Corset, J. Lambert, L. Pays, and P. Mehlen. 2012. Amyloid precursor protein regulates netrin-1-mediated commissural axon outgrowth. *J. Biol. Chem.* 287:30014–30023. http://dx.doi.org/10.1074/jbc.M111.324780

Richards, L.J., S.E. Koester, R. Tuttle, and D.D.M. O'Leary. 1997. Directed growth of early cortical axons is influenced by a chemoattractant released from an intermediate target. *J. Neurosci.* 17:2445–2458.

Rohde, M., M. Daugaard, M.H. Jensen, K. Helin, J. Nylandsted, and M. Jäättelä. 2005. Members of the heat-shock protein 70 family promote cancer cell growth by distinct mechanisms. *Genes Dev.* 19:570–582. http://dx.doi.org/10.1101/gad.305405

Serafini, T., T.E. Kennedy, M.J. Galko, C. Mirzayan, T.M. Jessell, and M. Tessier-Lavigne. 1994. The netrins define a family of axon outgrowth-promoting proteins homologous to *C. elegans* UNC-6. *Cell.* 78:409–424. http://dx.doi.org/10.1016/0092-8674(94)90420-0

Serafini, T., S.A. Colamarino, E.D. Leonardo, H. Wang, R. Beddington, W.C. Skarnes, and M. Tessier-Lavigne. 1996. Netrin-1 is required for commissural axon guidance in the developing vertebrate nervous system. *Cell.* 87:1001–1014. http://dx.doi.org/10.1016/S0092-8674(00)81795-X

Sharma, M., J. Burré, and T.C. Südhof. 2011. CSPα promotes SNARE-complex assembly by chaperoning SNAP-25 during synaptic activity. *Nat. Cell Biol.* 13:30–39. http://dx.doi.org/10.1038/ncb2131

Shekarabi, M., and T.E. Kennedy. 2002. The netrin-1 receptor DCC promotes filopodia formation and cell spreading by activating Cdc42 and Rac1. *Mol. Cell. Neurosci.* 19:1–17. http://dx.doi.org/10.1006/mcne.2001.1075

Shieh, J.C., B.T. Schaar, K. Srinivasan, F.M. Brodsky, and S.K. McConnell. 2011. Endocytosis regulates cell soma translocation and the distribution of adhesion proteins in migrating neurons. *PLoS ONE.* 6:e17802. http://dx.doi.org/10.1371/journal.pone.0017802

Shimura, H., D. Schwartz, S.P. Gygi, and K.S. Kosik. 2004. CHIP-Hsc70 complex ubiquitinates phosphorylated tau and enhances cell survival. *J. Biol. Chem.* 279:4869–4876. http://dx.doi.org/10.1074/jbc.M305838200

Srour, M., J.B. Rivière, J.M. Pham, M.P. Dubé, S. Girard, S. Morin, P.A. Dion, G. Asselin, D. Rochefort, P. Hince, et al. 2010. Mutations in *DCC* cause congenital mirror movements. *Science.* 328:592. http://dx.doi.org/10.1126/science.1186463

Südhof, T.C., and J.E. Rothman. 2009. Membrane fusion: grappling with SNARE and SM proteins. *Science.* 323:474–477. http://dx.doi.org/10.1126/science.1161748

Tcherkezian, J., and N. Lamarche-Vane. 2007. Current knowledge of the large RhoGAP family of proteins. *Biol. Cell.* 99:67–86. http://dx.doi.org/10.1042/BC20060086

Tessier-Lavigne, M., and C.S. Goodman. 1996. The molecular biology of axon guidance. *Science.* 274:1123–1133. http://dx.doi.org/10.1126/science.274.5290.1123

Turturici, G., G. Sconzo, and F. Geraci. 2011. Hsp70 and its molecular role in nervous system diseases. *Biochem. Res. Int.* 2011:618127. http://dx.doi.org/10.1155/2011/618127

Winkle, C.C., L.M. McClain, J.G. Valtschanoff, C.S. Park, C. Maglione, and S.L. Gupton. 2014. A novel Netrin-1–sensitive mechanism promotes local SNARE-mediated exocytosis during axon branching. *J. Cell Biol.* 205:217–232. http://dx.doi.org/10.1083/jcb.201311003

Yam, P.T., S.D. Langlois, S. Morin, and F. Charron. 2009. Sonic hedgehog guides axons through a noncanonical, Src-family-kinase-dependent signaling pathway. *Neuron.* 62:349–362. http://dx.doi.org/10.1016/j.neuron.2009.03.022

Yang, T., Y. Sun, F. Zhang, Y. Zhu, L. Shi, H. Li, and Z. Xu. 2012. POSH localizes activated Rac1 to control the formation of cytoplasmic dilation of the leading process and neuronal migration. *Cell Reports.* 2:640–651. http://dx.doi.org/10.1016/j.celrep.2012.08.007